Journal of Chromatography, 515 (1990) 91–123
Elsevier Science Publishers B.V., Amsterdam

CHROMSYMP. 1884

Fundamental study of hydroxyapatite high-performance liquid chromatography

II[a]. Experimental analysis on the basis of the general theory of gradient chromatography

TSUTOMU KAWASAKI*, MAKOTO NIIKURA and YURIKO KOBAYASHI
Chromatographic Research Laboratory, Koken Bioscience Institute, 3–5–18 Shimo-Ochiai, Shinjuku-Ku, Tokyo 161 (Japan)

ABSTRACT

In hydroxyapatite (HA) chromatography, competition occurs between the sample molecule and ions from the buffer for adsorption onto the crystal surface of HA. The competition mechanism for several proteins and nucleoside phosphates was analysed on the basis of the general theory of gradient chromatography that has been established recently. It was concluded that the number, x' of adsorbing sites of HA that are covered by an adsorbed molecule, in general, tends to increase slowly with increase in molecular mass, but that the correlation between molecular mass and x' is weak. The conclusion is consistent with the deduction made earlier that the stereochemical structure of the local molecular surface (which is highly characteristic of a molecule, and is intimately related to the x' value) is discerned by the regular crystal surface structure of HA. The capacity factor, k', is argued on the basis of the competition model.

INTRODUCTION

Hydroxyapatite [HA; $Ca_{10}(PO_4)_6(OH)_2$] column chromatography, a powerful technique for the separation of proteins, nucleic acids and viruses in aqueous systems, was originally introduced in 1956 by Tiselius *et al.*[2]. Between 1959 and the early 1970s, wa number of experiments were carried out by Bernardi's group with the purpose of elucidating the fundamental chromatographic mechanism. This was reviewed by Bernardi[3–5] and included the studies of other workers. In 1972, HA chromatography in the presence of a detergent was reported by Moss and Rosenblum[6]. In 1973–74, the

[a] For Part I, see ref. 1.

0021-9673/90/$03.50

interaction mechanism between nucleic acids and HA was explored by Martinson and Wagenaar (see, *e.g.*, refs. 7 and 8). In 1978, the chromatographic properties of several types of HA prepared by using different methods were studied by Spencer[9,10] in connection with both the crystal surface structure (as observed by scanning electron microscopy) and the size of the crystallites constituting the total HA particle (as deduced from the X-ray diffraction profile). In 1984, the experimental investigation that originated in Bernardi's laboratory was continued by Gorbunoff[11,12] and Gorbunoff and Timasheff[13]. In all the experiments above, open columns were used.

In 1983, stainless-steel columns for high-performance liquid chromatography (HPLC) packed with Tiselius type HA[2] were first commercialized by Bio-Rad Labs. (Richmond, CA, U.S.A.), followed by Koken (Tokyo, Japan), and accompanied with two publications[14,15]. Slightly retarded HPLC columns packed with coral HA (constructed by aggregation of hexagonal rods) were introduced by Mitsui Toatsu Chemicals (Tokyo, Japan). The first paper reporting an HPLC column packed with spherical HA with an average diameter of about 5 μm (constructed by aggregation of microcrystals) was published in 1986 by Kawasaki *et al.*[16], followed by a second paper[17]. Almost at the same time, an independent paper on a spherical HA packed HPLC column was published by Kadoya *et al.*[18]. In parallel with the appearance of these papers[16–18], spherical HA packed columns were introduced by Koken, Tonen (Tokyo, Japan) and Asahi Optical (Tokyo, Japan). In the first, besides HA particles as presented in refs. 16 and 17, those with average diameter of *ca.* 20 μm are also produced; HPLC columns packed with these particles are also available from Regis Chemical (Morton Grove, IL, U.S.A.). The last two columns contain HA particles as presented in ref. 18. About one year later, two other types of spherical HA packed column were introduced by Tosoh (Tokyo, Japan), followed by Cica-Merck (Tokyo, Japan); the first column was accompanied by a publication[19]. HPLC columns packed with square tile-shaped HA were also introduced by Koken, accompanied by a publication[20]. (Scanning electron micrographs of Tiselius type HA, spherical HA and square tile-shaped HA developed by Koken for HPLC and that of coral HA developed by Mitsui Toatsu Chemicals will be presented in Part III[21]).

An HPLC column packed with spherical particles of strontium phosphate HA $[Sr_{10}(PO_4)_6(OH_2]$ was developed by Kawasaki *et al.*[22] and a column packed with spherical particles of fluoroapatite $[Ca_{10}(PO_4)_6F_2]$ by Sato *et al.*[23].

A new method of separating acidic and basic proteins from each other by applying double gradients of KCl (or NaCl) and phosphate buffer was introduced by Kawasaki *et al.*[15] (see below). Recently, a novel technique of chromatographing uncharged glycoside molecules on an HA column in the presence of a high concentration (*e.g.*, 70–90%) of acetonitrile was introduced by Kasai *et al.*[24]. It can be deduced[25–27] that the adsorption and desorption mechanism occurring in the presence of acetonitrile is different from that interfering in the usual aqueous system both in the absence of acetonitrile and in the presence of the inorganic salt.

The study made in Part I[1] of this series[a] together with the analysis of

[a] Part I was presented 5 years ago at the Conference on Liquid Chromatography, Japan, wich will be published elsewhere[1]. The reasoning with respect to the fundamental chromatographic mechanisms (see later) will be considered in detail in ref. 1.

experimental data for open-column chromatography[3–5,11–13] leads to the following fundamental mechanisms of HA chromatography when carried out in an aqueous system. In general, two types of adsorbing surface appear on an HA particle packed in the column (to the precise, on the crystallites constituting an HA particle, the latter being a polycrystal or an assembly of polycrystals). On the first and the second surface, adsorbing sites (playing roles of anion and cation exchangers, called C and P sites) are arranged with minimum interdistances of the order of magnitude of the size of a crystal unit cell, respectively (for details, see Part III[21], where it will be shown that the first and second surfaces correspond to the **a** and the **c** crystal surface, respectively).

As far as the proteins are concerned, carboxyl groups on the molecular surface are used for the adsorption of a molecule onto C sites, and phosphate groups also act as adsorption groups onto C sites in the case of phosphoproteins. On the other hand, ε-amino and guanidinyl groups are used for the adsorption onto P sites. A protein molecule can therefore be adsorbed on HA in two different ways. Thus, in the first way, the molecule is adsorbed onto C sites (existing on the first or the **a** crystal surface) by using carboxyl (and phosphate) groups and, in the second, it is adsorbed onto P sites (existing on the second or the **c** crystal surface) by using ε-amino and guanidinyl groups. Following a statistical mechanical law, a canonical or a Boltzmann distribution is realized between the two modes of adsorption. In many actual instances, however, the Boltzmann distribution is biased towards one of the two extremes, and acidic proteins that have isoelectric points lower than 7 are adsorbed mainly onto C sites, whereas basic proteins that have isoelectric points higher than 7 are adsorbed mainly onto P sites. Nucleic acids or nucleotides are adsorbed onto C sites by using phosphate groups.

Phosphate ions from the potassium or sodium phosphate buffer (called the KP or the NaP buffer; for details of the KP buffer, see Experimental) are adsorbable onto C sites whereas potassium or sodium ions from the same buffer can be adsorbed only onto P sites. Therefore, in the presence of potassium or sodium phosphate buffer in the system, competition occurs between acidic proteins (or nucleotides) and phosphate ions and between basic proteins and potassium or sodium ions for adsorption onto C and P sites, respectively. In the competition mechanism, a number, x', of crystal sites (C or P) are generally covered by a sample molecule when it is adsorbed (to be precise, covered by a local surface, or local surfaces, of the molecule), whereas a single crystal site is covered by a competing ion (for details of the competition mechanism, see refs. 25–27).

With gradient chromatography using the KP or the NaP buffer to generate a molarity gradient, the sample molecules initially adsorbed at the inlet of the column forming a narrow band are driven out of the HA surface by competing ions from the molarity gradient; the development process thus proceeds.

Chloride ions, although they are anions, are virtually unadsorbable on the HA surface, presumably owing to steric hindrance. On the basis of this mechanism, the chromatographic behaviour, "acidic" or "basic", of an arbitrary molecule can be judged from a double gradient chromatographic experiment using double gradients of KCl and KP[15]. Fig. 1a illustrates a typical example of a double gradient chromatogram for a mixture of bovine serum albumin (BSA) (with pI = 4.7), cytochrome c (with pI = 9.8–10.1) and lysozyme (with pI = 10.5–11.0). This was obtained by previously applying the KCl gradient after an isocratic elution in the presence of a low

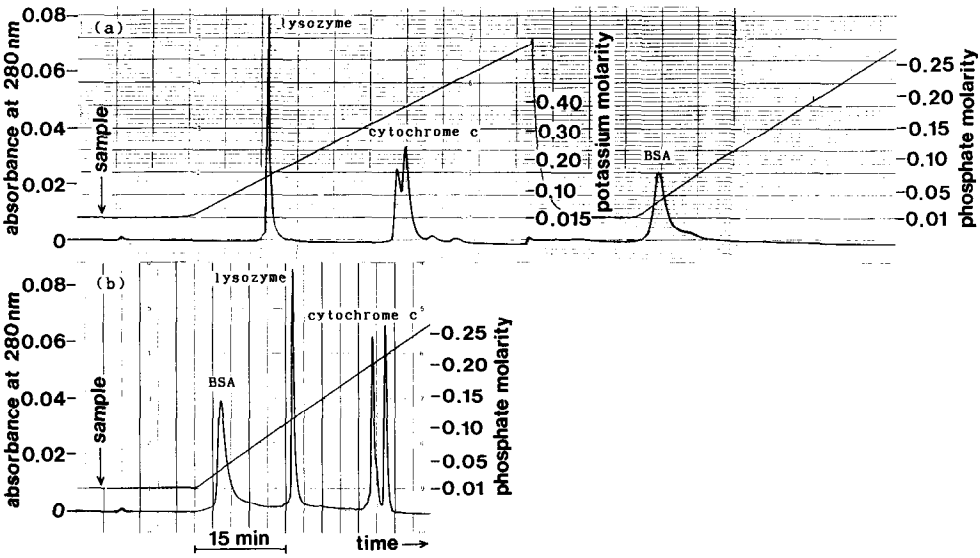

Fig. 1. (a) Double gradient chromatogram for a mixture of BSA (0.17 mg), cytochrome *c* (56 μg) and lysozyme (26 μg) as obtained on the KB column with ø = 6 mm and $L = 3 + 10 = 13$ cm) packed with spherical HA type S_2. Experimental conditions: $m_{in(P)} = 10$ m*M* for both KCl and KP gradients; $g'_{(KCl)} = 10.4$ m*M*/ml [$g'_{(KCl)}$ (ø = 1 cm) = 3.75 m*M*/ml]; $g'_{(P;KP)} = 6.94$ m*M*/ml [$g'_{(P;KP)}$ (ø = 1 cm) = 2.5 m*M*/ml]; flow-rate = 0.97 ml/min; $P = 1.8$–2.1 MPa; $T = 24.3$°C; recovery = 96%. (b) Single KP gradient chromatogram for a mixture of BSA (0.17 mg), cytochrome c (56 μg) and lysozyme (26 μg) as obtained on the same column. Experimental conditions: $m_{in(P)} = 10$ m*M*; $g'_{(P;KP)} = 6.94$ m*M*/ml [$g'_{(P;KP)}$ (ø = 1 cm) = 2.5 m*M*/ml]; flow-rate = 0.97 ml/min; $P = 1.8$–2.1 MPa; $T = 24.3$°C; recovery = 107%. For symbols, see Experimental and Results.

molarity (10 m*M*) of KP; 10 m*M* KP was present while the KCl gradient continued (left-hand side of Fig. 1a). The carrier solvent was again replaced with pure 10 m*M* KP, and the KP gradient was finally applied (right-hand side of Fig. 1a). It can be seen in Fig. 1a that BSA with an acidic p*I* is eluted in the second KP gradient whereas both cytochrome *c* and lysozyme with basic p*I* are eluted with the first KCl gradient. [It can be understood that the basic molecules (cytochrome *c* and lysozyme) that have been adsorbed on one of the two crystal surfaces (the **c** surface) are first desorbed and developed on the column, driven out of the crystal surfaces through competition with potassium ions from the first KCl gradient, while the acidic molecule (BSA) adsorbed on the other crystal surface (the **a** surface) remains on the crystal surfaces; the acidic BSA is hardly affected by the presence of the low molarity (10 m*M*) of KP and by the KCl gradient as chloride ions are virtually unadsorbable on both of the two types of crystal surface. BSA is desorbed from the HA surface (the **a** surface) and developed on the column, driven out of the crystal surfaces through competition with phosphate ions from the second KP gradient.] As a reference, a single KP gradient chromatogram for the same mixture is shown in Fig. 1b; this chromatogram is a superposition of the two chromatograms occurring in parallel on the basis of two different chromatographic mechanisms (see above).

The double gradient experiment was also performed for other molecules. It was confirmed that acidic molecules [DNA, ADP, ATP, adenosine tetraphosphate,

poly-L-aspartate, poly-L-glutamate, ovalbumin, pepsinogen and deoxyribonuclease I (DNase I)] are eluted in the second KP gradient whereas basic and neutral molecules [poly-L-lysine, poly-L-arginine, ribonuclease A (RNase A), trypsinogen, haemoglobin and myoglobin] are eluted in the first KCl gradient. In some instances with acidic and basic proteins, some minor components were eluted in the first KCl and the second KP gradient, respectively, however. The details of the experiments are published elsewhere[1] [in ref. 1, it was pointed out that the **a** surface of some commercially available spherical HA particles is damaged to a considerable extent. With these particles, acidic proteins are adsorbed so weakly on the **a** surface that the molecules are eluted from the column even before the second KP gradient begins in the double gradient system. In view of our experience, it is highly probable that the destruction of the surface structure occurred at least partially in the sintering process of microcrystals to make up a sphere (*cf.*, Part III[21])].

A molecule, in general, can take a number of different configurations on the crystal surface of HA. In other words, the molecule can be adsorbed using a number of different local surfaces, each of which can face the crystal surface and can orient in different directions on the crystal surface. Again following the statistical mechanical law, a Boltzmann distribution is realized among the configurations, and the energetically most stable adsorption configuration is realized with the highest probability (cf., eqn. 37 in ref. 25). In other words, the stereochemical structure of the local molecular surface (facing the crystal surface when the molecule is in the energetically most stable configuration) can be recognized by the regularity of the crystal surface structure of HA. As a results, the molecular separation highly characteristic of HA chromatography is realized. [In contrast to HA chromatography, with the usual ion-exchange chromatography the geometrical arrangement of the adsorbing sites (called ion exchangers) on the adsorbent would fluctuate microscopically among different loci in the column since the adsorbing sites are part of an organic substrate with a more or less flexible stereochemical structure. This implies that the energetically most stable configuration of a protein molecule adsorbed on the organic substrate varies among different loci in the column, and that the charges on the total molecular surface are used rather uniformly for the reaction with the adsorbent throughout a development process on the column. HA chromatography resembles affinity chromatography in that a subtle differene in the geometrical arrangement of atoms on a local molecular surface may be discriminated by the column owing to a *regular* stereochemical structure of the adsorbent surface.]

The points in Fig. 2 are experimental plots of eluent phosphate molarity [$m_{elu(P)}$] *versus* isoelectric point (p*I*) for 26 proteins obtained for open-column HA chromatography with both KP and NaP systems (reproduced from refs. 5, 11–13 and 28 with slight modifications[1]. The data for both KP and NaP systems have been plotted on a common [p*I*, $m_{elu(P)}$] plane as the experimental conditions (*i.e.*, both the total column length and the slope of the molarity gradient) that were applied were virtually identical for the two systems, and $m_{elu(P)}$ depends only slightly on the type of univalent cation involved in the buffer[1]. It can be seen in Fig. 2 that proteins that are not eluted from the column even in the presence of 3 *M* $CaCl_2$ (almost corresponding to "acidic" proteins that are eluted in the second KP gradient in the double gradient system; *cf.*, Appendix I in ref. 21; see also ref. 1) tend to be eluted at lower phosphate molarities than those which are eluted from the column in the presence of less than 10 m*M* $CaCl_2$ (almost

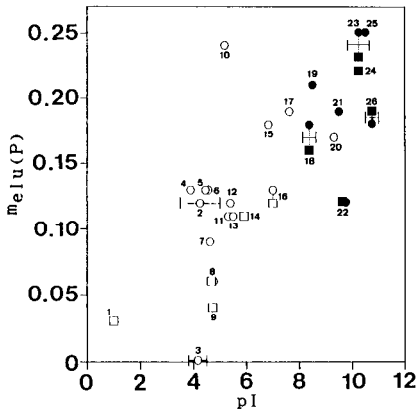

Fig. 2. Plots of $m_{elu(P)}$ *versus* p*I* for 26 proteins [1, pepsin; 2, Lima bean trypsin inhibitor; 3, ovamucoid; 4, pepsinogen; 5, soybean trypsin inhibitor; 6, α-lactalbumin; 7, ovalbumin; 8, bovine serum albumin; 9, deoxyribonuclease I; 10, β-lactoglobulin A; 11, carbonic anhydrase B; 12, catalase (bovine liver); 13, insulin; 14, snail acid deoxyribonuclease; 15, conalbumin; 16, myoglobin; 17, haemoglobin (horse); 18, α-chymotrypsin; 19, γ-chymotrypsin; 20, trypsinogen; 21, chymotrypsinogen; 22, ribonuclease A; 23, cytochrome *c*; 24, spleen acid deoxyribonuclease; 25, papaya lysozyme, 26, lysozyme (chicken)] obtained for open-column HA chromatography with both KP and NaP systems, where ø = 1 cm, *L* = 18–23 cm, $m_{in(P)}$ = 10 m*M* and $g'_{(P)}$ (ø = 1 cm) = 2.4–2.5 m*M*/ml (reproduced from refs. 5, 11–13 and 28 with slight modifications[1]; for symbols, see Experimental). ○ and □, "acidic" proteins that are not eluted from the column even in the presence of 3 *M* $CaCl_2$; ● and ■, "basic" proteins that are eluted in the presence of less than 10 m*M* $CaCl_2$; □ and ■, KP system; ○ and ●, NaP system.

corresponding to "basic" proteins that are eluted in the first KCl gradient in the double gradient system; *cf.*, Appendix I in ref. 21, see also ref. 1). Among the "acidic" and the "basic" proteins (*i.e.*, among the proteins obeying the same chromatographic mechanism), however, the correlation between $m_{elu(P)}$ and p*I* is very weak, respectively (see Fig. 2; also see Fig. 7 in Part III[21]).

The points in Fig. 3 are experimental plots (reproduced from ref. 29) of p*I* *versus* elution (or retention) time for a number of proteins obtained with a DEAE-5PW anion-exchange column (Tosoh) where a linear NaCl gradient was applied; the elution molarity, in general, increases linearly with an increase in elution time. It can be seen in Fig. 3 that elution time (elution molarity) is strongly correlated with p*I*.

Both Figs. 2 and 3 firmly support the deduction (see above) that the HA column discerns a stereochemical structure on a local surface of a protein molecule whereas the ion-exchange column is sensitive to the total charge per molecule. The possibility cannot be excluded, however, that, under certain circumstances where the secondary or the tertiary structure of the molecules under examination is fluctuating to a larger extent, a stronger correlation be realized between p*I* and elution molarity even in HA chromatography, In the special case when only the local molecular surface interfering in the reaction with the HA surface varies among the molecules under examination, a strong correlation might also be realized between p*I* and elution molarity.

Recently, a general theory of quasi-static linear gradient chromatography has been established for both small sample loads[30–32] and overloads[32–34]. Quasi-static chromatography is defined[32] as chromatography in which the rate of transition of a molecule between the mobile and the stationary phase is so high that the phase

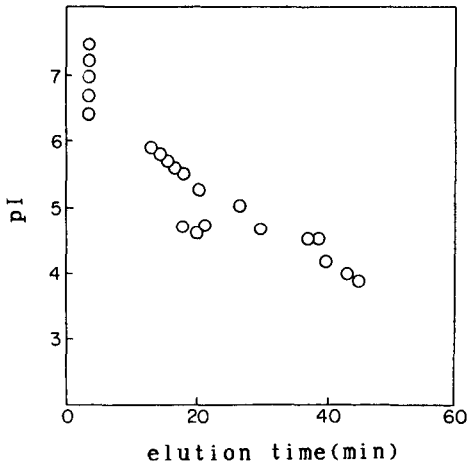

Fig. 3. Plots of p*I versus* elution time for a number of proteins obtained with an DEAE-5PW anion-exchange column of dimensions 10 cm × 0.78 cm I.D. (Tosoh). A linear NaCl gradient (0–0.4 *M*) was applied in the presence of 50 m*M* Tris–HCl buffer at pH 7.5 (reproduced from ref. 29).

transition effect hardly contributes to the longitudinal molecular diffusion in the column, and the longitudinal contribution of the Brownian diffusion occurring in the mobile phase is also negligible. From a practical point of view, the quasi-static condition can be assumed to hold in the usual HPLC. The fundamental structure of the theory with small sample loads is outlined schematically in the Appendix in ref. 32 (see also the first part of the Theoretical section in the presented work).

By introducing the competition mechanism (see above) into the general theory of quasi-static linear gradient chromatography, a concrete theoretical chromatogram can be calculated[30,34].

Experimental verifications of the theory of gradient chromatography into which the competition model is introduced have been made for HA chromatography carried out under both small-load[34–37] and overload[34,38] conditions. The significance of these studies is that the competition mechanism in HA chromatography has been verified on quantitative basis.

In this paper, the chromatographic behaviour of several basic and acidic proteins and nucleoside phosphates under small-load conditions on a spherical HA packed HPLC column is analysed on the basis of the theory of gradient chromatography into which the competition model is introduced. From the analysis, the adsorption configuration of the molecules on the crystal surface of HA can be deduced. Further experimental verifications of the competition model itself are added.

Most of the experimental data that were used for the analysis are original; however for some analyses, data published in earlier papers are reused (the abbreviations that are used in this paper are as follows: HA, hydroxyapatite; HPLC, high-performance liquid chromatography; ø, inside column diameter; KP or NaP, potassium or sodium phosphate buffer, respectively, at pH $\approx$ 6.8; *P*, pressure drop; *T*, temperature; RNase A, ribonuclease A; IgG, immunoglobulin G; DNase I, deoxyribonuclease I; BSA, bovine serum albumin).

THEORETICAL

General theory of quasi-static linear gradient chromatography with small sample loads[30–32]

Let us consider quasi-static linear gradient chromatography with small sample loads when a band of the sample molecules with an infinitesimal width is initially formed at the inlet of the column. When both the slope, g, of the molarity gradient and the total length, L, of the column are given, the theoretical chromatogram, f, for a molecular component under consideration in the sample mixture can, in general, be represented as a function of molarity, m, in the molarity gradient by eqn. 43 in ref. 30. This can be rewritten with slight modifications as

$$f(m) = \frac{1}{\sqrt{2\pi}\ \sigma(s;g)} \cdot \exp\left\{ - \frac{[m-\mu(s)]^2}{2[\sigma(s;g)]^2} \right\} \tag{1}$$

where

$$s = \int_{m_{in}}^{\mu} \frac{B'(m)}{1 - B'(m)} \cdot \mathrm{d}m \tag{2}$$

by which the function $\mu(s)$ is implicitly defined, and

$$\sigma(s;g) = \frac{\sqrt{2g\Theta_0 s}}{B'[\mu(s)]} \tag{3}$$

The physical meanings of the symbols involved in eqns. 1–3 are as follows:

g = slope of the molarity gradient expressed as the increase in molarity per unit length of the column measured from the outlet to the inlet of the column. (In earlier papers[30–32], the slope, g', of the gradient expressed as the increase in molarity per unit interstitial volume of the column was considered instead of g.)

s = parameter representing the difference in molarity between the inlet and the outlet of the column, defined as the product of g and the total length, L, of the column:

$$s = gL \tag{4}$$

(In refs. 30–32, s was defined as the product of g' and the total interstitial volume, L', of the column. It is evident that $g'L'$ is equal to gL.)

m_{in} = initial molarity at the beginning of the molarity gradient.

Θ_0 = parameter with the dimensions of length that measures the longitudinal diffusion in the column. Θ_0 depends on the g value, the type of sample molecule and the type of solvent except in an ideal case (see ref. 31). Θ_0 is intimately related to the plate height concept[39]. (In refs. 30–32, the parameter $\Theta \equiv \Theta_0 g/g'$ was considered instead of Θ_0.)

$\mu(s)=$ elution molarity at the centre or the maximum height of the chromatographic peak, which can be considered to be a function of s (*cf.*, eqn. 2).

$\sigma(s;g)=$ standard deviation (with the dimensions of molarity) of the chromatographic peak measured in terms of the molarity range of the gradient over which the peak appears. σ can be considered to be a function of s involving the parameter g (*cf.*, eqn. 3).

$B'(m)=$ partition of sample molecules (of the chromatographic component under consideration) in the mobile phase in an elementary volume of the column in which the molarity of the gradient element is m. B', in general, increases monotonically from *ca.* 0 to 1 with increase in m. B' is related to the capacity factor, k', by the relationship $B' = 1/(1 + k')$ or $k' = (1 - B')/B'$ (*cf.*, eqn. 8).

Theory into which the competition model is introduced[30]

On the basis of the competition model where it is assumed that the adsorption of a sample molecule occurs on a single type of the adsorbent surface, the function $B'(m)$ under small-load conditions can be represented by eqn. 29 in ref. 27 (i.e., eqn. 44 in ref. 30) as

$$B'(m) = \frac{1}{1 + q \cdot (\varphi m + 1)^{-x'}} \tag{5}$$

$m=$ molarity of competing ions.

$\varphi=$ positive constant characterizing the competing ions constituting the molarity gradient. This measures the strength of adsorption of the ions onto the adsorbent surface (*cf.*, eqns. 18 and 21 in ref. 27).

$q=$ positive constant characterizing the sample molecule under consideration. This measures the strength of adsorption of the molecule on the adsorbent surface [*cf.*, eqn. 27 in ref. 27, where q is written as $q_{(\rho')}$].

$x'=$ number of adsorbing sites on the adsorbent surface covered by an adsorbed sample molecule, i.e., the number of sites on which the adsorption of competing ions is impossible owing to the presence of an adsorbed sample molecule, or the number of competing ions the adsorption of which is impossible owing to the presence of an adsorbed sample molecule. (Eqn. 5 was derived[25–27] on the basis of the assumption that a single site is covered by a competing ion when it is adsorbed. Eqn. 5 holds approximately even in the absence of this assumption, however. In this instance, the parameter x' has only the last physical meaning of the number of competing ions the adsorption of which is impossible owing to the presence of an adsorbed sample molecule.)

The prototype of eqn. 5 was first derived in an earlier paper[40], and a most reasonable method for its derivation on the basis of a grand canonical ensemble has been published recently[25–27]. The function $B'(m)$ in which account is taken of the possibility that a sample molecule can be adsorbed on two types of adsorbent surface was derived in ref. 41. However, this function is not applied here.

By introducing eqn. 5, both eqns. 2 and 3 can be rewritten concretely as

$$\mu(s) = \frac{1}{\varphi}\{[(x' + 1)\varphi q s + (\varphi m_{in} + 1)^{x'+1}]^{1/(x'+1)} - 1\} \quad (6)$$

and

$$\sigma(s;g) = \sqrt{2g\Theta_0 s}\,\{1 + q[\varphi\mu(s) + 1]^{-x'}\} \quad (7)$$

respectively. (Eqn. 6 was originally derived as eqn. 15 in ref. 35 on the basis of a primitive consideration. Eqns. 6 and 7 appear as eqns. 45 and 46, respectively, in ref. 30.)

Finally, the capacity factor, k', as a function of m can be represented by

$$k'(m) = q(\varphi m + 1)^{-x'} \quad (8)$$

(*cf.*, eqn. 5).

EXPERIMENTAL AND RESULTS

Materials and methods

Both spherical HA particles (type S_1 or S_2 with diameters of about 5 μm; see Fig. 2b in ref. 21 for HA type S_1) and HA-packed SUS316 stainless-steel columns (KB columns; Koken) were prepared in our laboratory. [Type S_1 and S_2 particles are almost identical. Except for two experiments carried out using HA type S_2 (Fig. 1), HA type S_1 was used.] Except for one case (see below), the column I.D. was 6 mm; lengths of 0.5, 1, 3, 10 and 30 cm were prepared. The 3-cm column was used as either a precolumn or a main column. If a large overall column length was necessary , it was provided by connecting 30-cm columns in series by using fine tubes. For the purpose of preparing three components of IgG, a column of I.D. 2 cm and length 5 cm was used (see Appendix II).

The HPLC experiments were carried out at room temperature by connecting the column (or the column system) to an HPLC pump. Thus, with gradient chromatography, the sample molecules dissolved in 1 m*M* potassium phosphate buffer at pH $\approx$ 6.8 (*i.e.*, an equimolar mixture of K_2HPO_4 and KH_2PO_4; called KP buffer. 1 m*M* relates to phosphate ions in the KP buffer) was injected into the column (or the column system) by using an injector located between the HPLC pump and the column inlet; this was followed by rinsing with 1 m*M* KP buffer. During this process, virtually all the molecules (except denatured minor components) remained in the stationary phase (*i.e.*, on the surface of the adsorbent) in the vicinity of the column inlet forming a band. Material was then eluted using a linear molarity gradient of KP buffer. The sample elution was monitored by measuring the ultraviolet absorption (at 230, 260, 280 or 415 nm) in a flow cell. At the same time, the molarity gradient was monitored by measuring the refractive index in a special flow cell with a low angle.

With isocratic chromatography, which was carried out for the purpose of determining the R_F or the B' value of the sample molecule occurring in the presence of

KP buffers with different constant molarities, a pulse band of sample molecules was injected into two column systems with overall lengths of 13 (= 3 + 10) and 33 (= 3 + 30) cm. The difference in elution volumes at the maximum height of the molecular band between the two systems was measured. The R_F value was calculated as the ratio of the void volume involved in the column length of 20 (= 33 − 13) cm to the difference in elution volumes (for the void volume, see below). The R_F value should be virtually equal to B' (*cf.*, the "first principle of chromatography in general" mentioned in Appendix III in ref. 30).

The experiment for the determination of the void volume of the column was also carried out by connecting columns (or column systems) with several overall lengths to the HPLC pump, and the pulse sucrose band dissolved in 1 m*M* KP was developed by using 1 m*M* KP as the solvent; the elution of the sucrose band was detected by measuring the refractive index in the flow cell.

The sample molecules applied in the HPLC experiments were lysozyme (from chicken egg white; P-L Biochemicals), lysozyme (from turkey egg white; Sigma), cytochrome c (from horse heart; Sigma), ribonuclease A (from bovine pancreas; Sigma), trypsinogen (from bovine pancreas; Sigma), haemoglobin (human; a gift from the Institute for Adult Diseases, Asahi Life Foundation, Tokyo, Japan), immunoglobulin G (human, with isoelectric points between 6.5 and 9; Japanese Red Cross Plasma Fractionation Centre, Tokyo, Japan), myoglobin (from sperm whale skeletal muscle; Sigma), deoxyribonuclease I (from bovine pancreas; Millipore), albumin (from bovine serum; Nutritional Biochemicals), ovalbumin (from chicken egg white; Sigma), pepsinogen (from hog stomach mucosa; Tokyo Kasei Kogyo), ADP (Sigma), ATP (Sigma) and adenosine tetraphosphate (Sigma).

Determination of the void volume of the column

The volume of the solvent (1 m*M* KP) at which a pulse of sucrose solution (dissolved in 1 m*M* KP) is eluted was measured by using HA columns with different overall lengths. On the basis of this experiment, the ratio of the void volume to the total packed volume of the HA crystals in the column was calculated to be 0.823, assuming that the migration velocity of sucrose is equal to that of the solvent.

Important experimental parameters in gradient chromatography

Before giving the results of the HPLC experiments (see the next sub-section), it is necessary to define important experimental parameters, as follows.

$m_{(P)}$ and $m_{(K^+)}$: phosphate and potassium molarities in the KP buffer, respectively. $m_{(K^+)}$ is 1.5 times $m_{(P)}$. With "acidic" molecules that compete with phosphate ions from the KP buffer for adsorption onto C sites, m (see eqns. 1, 2 and 5) represents $m_{(P)}$, *i.e.*,

$$m = m_{(P)} \tag{9}$$

With "basic" molecules that compete with potassium ions from the KP buffer for adsorption onto P sites, m represents $m_{(K^+)}$, *i.e.*,

$$m = m_{(K^+)} = 1.5m_{(P)} \tag{9'}$$

$m_{elu(P)}$: elution phosphate molarity, *i.e.*, the phosphate molarity in the KP gradient at which the maximum height of the chromatographic peak is eluted. With "acidic" and "basic" molecules, μ (eqn. 6) can be represented in terms of $m_{elu(P)}$ by the relationships

$$\mu = m_{elu(P)} \tag{10}$$

and

$$\mu = 1.5m_{elu(P)} \tag{10'}$$

respectively.

$m_{in(P)}$: initial phosphate molarity, *i.e.*, the phosphate molarity in the KP buffer occurring before the KP gradient begins. With "acidic" and "basic" molecules, m_{in} (eqn. 6) can be represented in terms of $m_{in(P)}$ by the relationships

$$m_{in} = m_{in(P)} \tag{11}$$

and

$$m_{in} = 1.5m_{in(P)} \tag{11'}$$

respectively.

$\sigma_{(P)}$: standard deviation (with the dimensions M or mM) of the chromatographic peak measured in terms of the phosphate molarity range of the KP gradient over which the peak appears. With "acidic" and "basic" molecules, σ (eqn. 7) can be represented in terms of $\sigma_{(P)}$ by the relationships

$$\sigma = \sigma_{(P)} \tag{12}$$

and

$$\sigma = 1.5\sigma_{(P)} \tag{12'}$$

respectively. For practical purposes, $\sigma_{(P)}$ is represented here as the half-width at 0.6065 times the maximum height of the experimental peak; this is identical with the standard deviation provided that the peak has a precise Gaussian shape.

L: total (overall) column length measured in centimeters.

$g'_{(P)}$ ($\varnothing = 1$ cm): reduced slope (to inside column diameter $\varnothing = 1$ cm) of the phosphate gradient [with a slope $g'_{(P)}$] in the KP gradient, measured in units of M/ml or mM/ml. $g'_{(P)}$ ($\varnothing = 1$ cm) is 0.36 ($=0.6^2$) times as large as $g'_{(P)}$ when the column of I.D. 6 mm is used for the experiment. With "acidic" and "basic" molecules, g (eqn. 4) measured in units of M/cm or mM/cm can be represented in terms of $g'_{(P)}$ ($\varnothing = 1$ cm) by the relationships:

$$\begin{aligned} g &= (\pi/4) \cdot 0.823 \cdot g'_{(P)} \ (\varnothing = 1 \text{ cm}) \\ &= 0.646g'_{(P)} \ (\varnothing = 1 \text{ cm}) \end{aligned} \tag{13}$$

and

$$g = (\pi/4) \cdot 0.823 \cdot 1.5 \cdot g'_{(P)} \ (\varnothing = 1 \text{ cm})$$
$$= 0.970 g'_{(P)} \ (\varnothing = 1 \text{ cm}) \qquad (13')$$

respectively, where 0.823 represents the ratio of the void volume to the total packed volume of the HA crystals in the column that has been determined in the previous sub-section. [Similarly, the slope and the reduced slope of the KCl gradient are represented by $g'_{(KCl)}$ and $g'_{(KCl)}$ ($\varnothing = 1$ cm), respectively ;*cf.*, Figs. 1 and 16.]

$s_{app(P)}$: product of $g'_{(P)}$ ($\varnothing = 1$ cm) and L. With "acidic" and "basic" molecules, s (eqn. 4) can be written in terms of $s_{app(P)}$ as

$$s = 0.646 s_{app(P)} \qquad (14)$$

and

$$s = 0.970 s_{app(P)} \qquad (14')$$

respectively.

$q_{app(P)}$: experimental parameter related to q (eqns. 5–7) by the relationships

$$q = q_{app(P)}/0.646 \qquad (15)$$

and

$$q = q_{app(P)}/0.970 \qquad (15')$$

with "acidic" and "basic" molecules, respectively.

The parameters φ, x' and Θ_0 in eqns. 5–7 are also used as experimental parameters. φ characterizes competing phosphate and potassium ions with chromatography of "acidic" and "basic" molecules, respectively; x' represents either the number of C sites covered by an "acidic" molecule, or the number of P sites covered by a "basic" molecule; except in an ideal case, Θ_0 depends on the g value, the type of sample molecule and the type of competing ion (see ref. 31).

Results of HPLC experiments

The samples applied in the HPLC experiments are listed in Table I, of which proteins 1–10 behave as "basic" molecules, eluted from the column with the first KCl gradient in the double gradient system; proteins 11–18 and nucleoside phosphates 19–21 behave as "acidic" molecules, eluted with the second KP gradient in the system (for the double gradient system, see Introduction). [For details, see Part I[1], where it should be recalled that myoglobin behaves partially as an "acidic" molecule in effect as the elution molarity in the KCl gradient in the double gradient system is considerably higher than the elution molarity in the KP gradient in the single gradient system (*cf.*, Appendix I in ref. 21). For the sake of convenience, however, here we analyse the myoglobin data assuming that the protein behaves as a "basic" molecule. In connection with this problem, myoglobin (and also horse haemoglobin and trypsinogen with isoelectric points higher than 7, respectively) behaves as an "acidic"

TABLE I

SUMMARY OF RESULTS OF GRADIENT HPLC EXPERIMENTS CARRIED OUT USING A VALUE OF THE PARAMETER ϕ OF 25 M^{-1}

No.	*Protein or nucleoside phosphate*	*Isoelectric point*	*Molecular mass (kDa)*	*Chromatographic behaviour*[a]	*x'(l.l.,u.l.)*[b]	*Ln $q_{app(P)}$*	*Ln q*	*$\dot{m}_{(P)}$*[c] *(M)*	*$m_{elu(P)}$*[d] *(M)*	*$\Theta_0(cm)$*[e]				*Fig. No.*
										5.0[f]	*2.5*[f]	*1.25*[f]	*0.45*[f]	
1	Lysozyme (chicken)	10.5–11.0	14.3	Basic	5.7 (4.0, 8.0)	9.5	9.5	0.115	0.113	0.004	0.005	0.008	0.013	4
2	Lysozyme (turkey)		14.2	Basic	5.7 (4.5, 8.0)	10.1	10.1	0.130	0.132		0.005	0.008		
3	Cytochrome *c* (in reduced state)[g]	9.8–10.6	11.7	Basic	4.8 (4.0, 6.0)	11.2	11.2	0.248	0.212	0.004	0.005	0.005	0.010	5
4	Cytochrome *c* (in oxidized state)[h]			Basic	4.8 (3.9, 6.0)	10.8	10.8	0.226	0.202					
5	RNase A[i]	9.7	13.7	Basic	4.3 (2.7, 6.7)	6.9	6.9	0.106	0.112		0.003		0.015	
6	Trypsinogen[i]	9.3	24.0	Basic	5.2 (3.5, 7.5)	7.7	7.7	0.091	0.097					
7	Haemoglobin[i]	7.0	64.5	Basic	5.7 (3.7, 8.0)	8.2	8.2	0.086	0.085					
8	IgG (fraction I)[j]		153	Basic	11.0 (6.4, 20.0)	11.2	11.2	0.047	0.052					6
9	IgG (fraction II)[j]		153	Basic	11.0 (8.0, 15.0)	16.6	16.6	0.094	0.099					
10	Myoglobin[i]	7.0	17.2	Basic	4.3 (2.8, 6.1)	6.6	6.6	0.097	0.093		0.010		0.020	
11	DNase I[k] (peak I)	4.7	28.7	Acidic	8.0 (2.0, 18.0)	2.0	2.4	0.014	0.020					
12	DNase I[k] (peak 2)			Acidic	5.0 (2.1, 8.5)	3.5	3.9	0.047						
13	DNase I (peak 3)			Acidic	5.5 (3.3, 8.0)	6.3	6.7	0.095						
14	DNase I (peak 4)			Acidic	6.0 (4.1, 8.5)	8.7	9.1	0.142	0.147					

15	BSA	4.7	66.3	Acidic	6.0	(2.5, 12.0)	3.6	4.0	0.038	0.049		0.23[l]	0.30[l]	0.50[l]	7
16	Ovalbumin[i]	4.6	43.5	Acidic	8.0	(2.0, 23.0)	0.5	0.9	0.005	0.015					
17	Pepsinogen[i]	3.9	40.4	Acidic	7.0	(2.5, 15.0)	3.7	4.1	0.032	0.046					
18	IgG (fraction III)[j]		153	Acidic	18.0	(14.0, 27.0)	25.0	25.4	0.124	0.131					8
19	ADP		0.4	Acidic	2.5	(1.2, 5.0)	2.0	2.4	0.064	0.050	0.07	0.10	0.15	0.25	9
20	ATP		0.5	Acidic	2.5	(1.2, 3.5)	4.2	4.6	0.212	0.137					
21	Adenosine tetraphosphate		0.6	Acidic	2.5	(2.0, 3.5)	5.7	6.1	0.419	0.228					

[a] This was judged from the double gradient chromatography experiment using double gradients of KCl and KP (see Introduction).

[b] l.l. and u.l. represent the lower and the upper limit value of x' (*i.e.*, $x'_{l.l}$ and $x'_{u.l.}$), respectively; see Appendix I.

[c] See Appendix III.

[d] Elution phosphate molarity obtained experimentally when L = 13 cm and $g'_{(P)}$ (ϕ = 1 cm) = 2.5 mM/ml. The average value is shown when several experiments were repeated (*cf.*, Appendix III).

[e] The Θ_0 value was not calculated for chromatographic peaks in which highly heterogeneous substances are involved or those in which molecular degradation is in progress to a large extent [both cases with ATP and adenosine tetraphosphate; *cf.*, ref. 1 and first sub-section of Discussion).

[f] The $g'_{(P)}$ (ϕ = 1 cm) value (in units of mM/ml) that was applied.

[g] This is involved in the second peak of the double peak chromatogram (*cf.*, ref. 16).

[h] This is involved in the first peak of the double peak chromatogram (*cf.*, ref. 16).

[i] Analysis was performed for the main peak of the chromatogram.

[j] See Appendix II.

[k] Peak 1 is the main peak; see Fig. 5 in ref. 17. The experiments were carried out by using column systems with overall lengths of 13 (= 3 + 10) and 33 (= 3 + 30) cm[17]. The precolumn part (with a length of 3 cm) of the systems, however, was packed with square tile-shaped HA or HA type F, the main part being packed with HA type S_1 (see ref. 17; for square tile-shaped HA or HA type F, see Fig. 2d in Part III[21]).

[l] The high value of Θ_0 is apparent, arising from the fact that several components are involved in a chromatographic peak.

molecule in the $CaCl_2$ system (*cf.*, Apendix I in ref. 21). It should also be noted that some "basic" components are contaminating "acidic" DNase I. The experimental analyses for RNase A, trypsinogen, haemoglobin, myoglobin, ovalbumin and pepsinogen will be performed for the main peak of the chromatogram.

The points in Fig. 4a are experimental plots (reproduced from ref. 34 of $m_{elu(P)}$ *versus* L for chicken lysozyme for four different $g'_{(P)}$ (ø = 1 cm) values, 5.0, 2.5, 1.25 and 0.45 mM/ml. It can be seen that the profile of the experimental plot is parallel with those obtained for Tiselius type HA packed columns[35–37,42]; $m_{elu(P)}$ increases with increasing L and $g'_{(P)}$ (ø = 1 cm) when $g'_{(P)}$ (ø = 1 cm) and L are constant, respectively. The dependence of $m_{elu(P)}$ on L differs when the $g'_{(P)}$ (ø = 1 cm) applied is

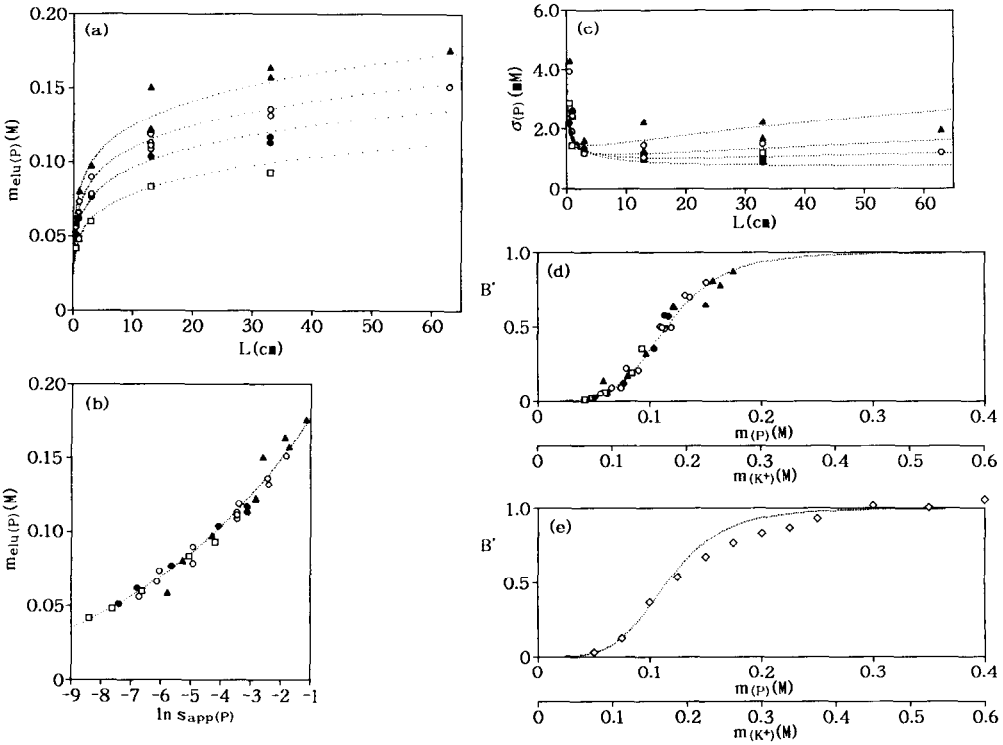

Fig. 4. Analysis of HPLC for chicken lysozyme. Points in (a)–(d): experimental plots of (a) $m_{elu(P)}$ *versus* L, (b) $m_{elu(P)}$ *versus* ln $s_{app(P)}$, (c) $\sigma_{(P)}$ *versus* L and (d) B' *versus* $m_{(P)}$ or $m_{(K^+)}$ for four different $g'_{(P)}$ (ø = 1 cm) values: (▲) 5.0, (○) 2.5, (●) 1.25 and (□) 0.45 mM/ml; the corresponding sample loads are 16–30, 20–60, 30 and 50 μg. Curves in (a)–(d): theoretical curves calculated by using (a) eqn. 6, (b) eqn. 6, (c) eqn. 7 and (d) eqn. 5; in the equations, the parameters m, μ, m_{in}, σ, g, s and q have been represented in terms of $m_{(P)}$, $m_{elu(P)}$, $m_{in(P)}$, $\sigma_{(P)}$, $g'_{(P)}$ (ø = 1 cm), $s_{app(P)}$ and $q_{app(P)}$ by using eqns. 9′–15′, respectively. With regard to the invariable parameters that are involved in the equations, the numerical values that were used for the calculation are listed in Table I. [Both the experimental plots and the theoretical curves in (a) and (b), and those for $g'_{(P)}$ (ø = 1 cm) = 2.5 mM/ml in (c) have been reproduced from ref. 34. The experimental conditions in (a)–(d) are indicated in ref. 34, where the dependence of $m_{elu(P)}$ and $\sigma_{(P)}$ on both flow-rate and sample load are also shown.] Points in (e): experimental plots of B' *versus* $m_{(P)}$ or $m_{(K^+)}$, where B' values have been estimated from isocratic chromatography carried out under the following experimental conditions: flow-rate, 0.48–0.50 ml/min; P, 1.6–5.9 MPa; T, 22.5–27.0°C. Curve in (e): theoretical curve identical with that shown in (d).

different, giving four arrangements of the experimental points corresponding to the four values of $g'_{(P)}$ ($\varnothing = 1$ cm) (see Fig. 4a).

The points in Fig. 4b are plots of $m_{elu(P)}$ *versus* ln $s_{app(P)}$ instead of L for the experimental points in Fig. 4a. It can be seen that the four arrangements of the experimental points on the [L, $m_{elu(P)}$] plane (Fig. 4a) converge into a single arrangement when mapped on the [ln $s_{app(P)}$, $m_{elu(P)}$] plane.

The curve in Fig. 4b is theoretical, calculated by using eqn. 6 in which the term qs has been replaced by $q_{app(P)}s_{app(P)}$ by using both eqns. 14′ and 15′, and $m_{in} = 1.5$ mM since $m_{in(P)} = 1$ mM (see eqn. 11′). For $\varnothing$, the optimum value, 25 M^{-1}, has been used (see Appendix I); this value will hereafter be used for all the calculations. For the other parameters, x' and $q_{app(P)}$, values that are shown in Table I have been applied in order to obtain a best fit with the experiment. It can be seen in Fig. 4b that the coincidence of the theoretical curve with the experimental plot is excellent, explaining a slight displacement from linearity of the arrangement of the experimental points.

The four curves in Fig. 4a were obtained by mapping the theoretical curve in Fig. 4b on the [L, $m_{elu(P)}$] plane when $g'_{(P)}$ ($\varnothing = 1$ cm) = 5.0, 2.5, 1.25 and 0.45 mM/ml, respectively.

The points in Fig. 4c are experimental plots of $\sigma_{(P)}$ *versus* L for the four $g'_{(P)}$ ($\varnothing =$ 1 cm) values in Fig. 4a where the same experimental data as used in both Fig. 4a and b were applied. The curves in Fig. 4c are theoretical, calculated by using eqn. 7 with reference to eqns. 12′, 13′, 14′ and 15′; for the values of the parameters involved in eqn. 7, those which are shown in Table I were applied in order to obtain the best fits with the experiment.

The curve in Fig. 4d is theoretical, representing B' for chicken lysozyme as a function of $m_{(P)}$ or $m_{(K^+)}$. This was calculated by using eqn. 5 in which the values of the parameters that are shown in Table I were applied. The points in Fig. 4d correspond to the experimental points in Fig. 4a or b. Hence the theoretical curve in Fig. 4b performs a parallel transition in the abscissa direction when q or $q_{app(P)}$ varies in eqn. 6 (*cf.*, Appendix I). Therefore, the value of the parameter q which superimposes the curve on each experimental point can be estimated. By using this q value, and replacing $m_{elu(P)}$ with $m_{(P)}$ (with reference to both eqns. 9′ and 10′), B' (eqn. 5) was calculated, and the position of any point in Fig. 4d was determined.

It also is possible to calculate B' values from R_F values that are obtained from isocratic chromatography carried out by using buffers with different constant molarities $m_{(P)}$ or $m_{(K^+)}$ (see the first sub-section). The points in Fig. 4e are experimental plots of B' for chicken lysozyme *versus* $m_{(P)}$ or $m_{(K^+)}$ obtained by using this method. In Fig. 4c, the theoretical curve in Fig. 4d is reproduced.

Figs. 5 and 6 represent both experimental plots and theoretical curves that correspond to those in Fig. 4 for other "basic" proteins: cytochrome *c* (in reduced state; Fig. 5) and fractions I and II of IgG (Fig. 6) (for IgG, see Appendix II).

Figs. 7–9 are concerned with "acidic" molecules: BSA (Fig. 7), fraction III of IgG (Fig. 8; *cf.*, Appendix II) and ADP (Fig. 9).

Fig. 10 represents mappings onto both {$m_{(P)}$ [or $m_{(K^+)}$], ln k'} and {ln $m_{(P)}$ [or ln $m_{(K^+)}$], ln k'} planes of both the experimental points and the theoretical curves (calculated by using eqn. 8) for all the samples listed in Table I.

In Table I, the analytical results of all the experiments are summarized. Figs. 11 and 12 represent plots of x' *versus* molecular mass for "basic" and "acidic" substances, respectively, that are shown in Table I.

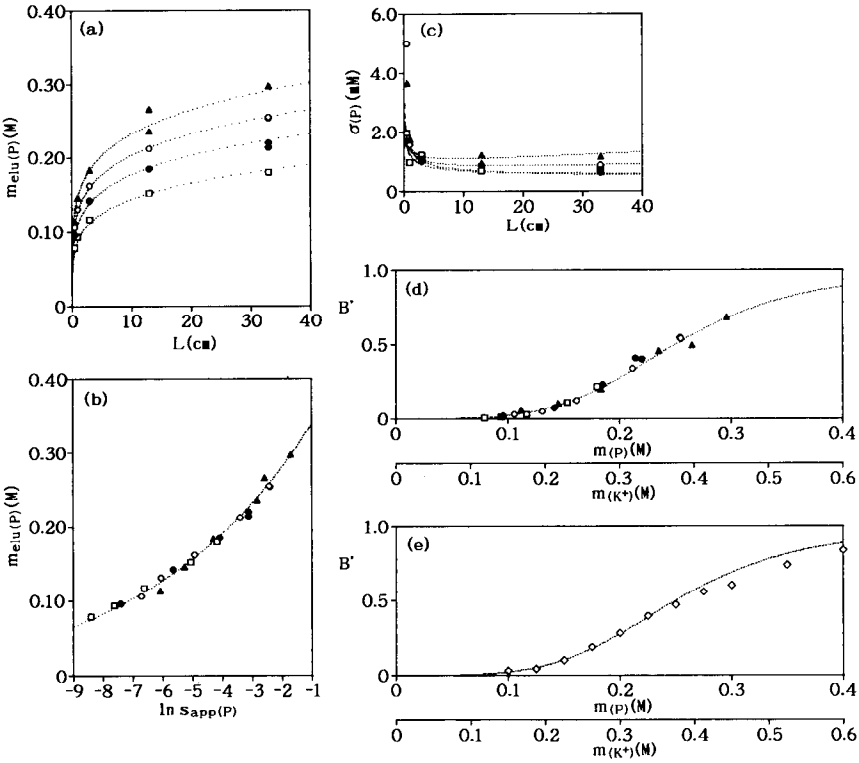

Fig. 5. Analysis of HPLC for cytochrome *c* in reduced state. The experiment was carried out by using the sample in which both molecules in reduced and oxidized states are involved. Points in (a)–(d): experimental plots of (a) $m_{clu(P)}$ *versus* *L*, (b) $m_{clu(P)}$ *versus* ln $s_{app(P)}$, (c) $\sigma_{(P)}$ *versus* *L* and (d) *B'* *versus* $m_{(P)}$ or $m_{(K^+)}$ for four different $g'_{(P)}$ (ø = 1 cm) values: (▲) 5.0, (○) 2.5, (●) 1.25 and (□) 0.45 m*M*/ml; the corresponding total sample loads are 32–60, 40–120, 50–60 and 100–300 μg. Other experimental conditions: $m_{in(P)}$ = 1 m*M*; flow-rate, 0.46–0.51 ml/min; *P*, 0.3–5.2 MPa; *T*, 21.0–29.7°C. Curves in (a)–(d): theoretical curves calculated by using (a) eqn. 6, (b) eqn. 6, (c) eqn. 7 and (d) eqn. 5; for details of the calculation method, see the legend for Fig. 4a–d. Points in (e): experimental plots of *B'* *versus* $m_{(P)}$ or $m_{(K^+)}$, where *B'* values were estimated from isocratic chromatography carried out under the following experimental conditions: flow-rate, 0.49–0.50 ml/min; *P*, 1.7–5.4 MPa; *T*, 24.2–26.5°C. Curve in (e): theoretical curve identical with that shown in (d).

DISCUSSION

General discussion

Both Figs. 11 and 12 show a tendency for the number, *x'*, of crystal sites (P or C) that are covered by an adsorbed molecule to increase with increase in molecular mass. The increase occurs slowly, however, and the correlation between molecular mass and *x'* is weak (Figs. 11 and 12). The weak correlation is consistent with the deduction that the stereochemical structure of the local molecular surface (which is highly characteristic of a molecule, and is intimately related to the *x'* value) is discerned by the regular crystal surface structure of HA [see Introduction; *cf.*, Fig. 2 here and Fig. 7 in Part III[21]].

The slow increase in *x'* with increase in molecular mass (see above) shows that

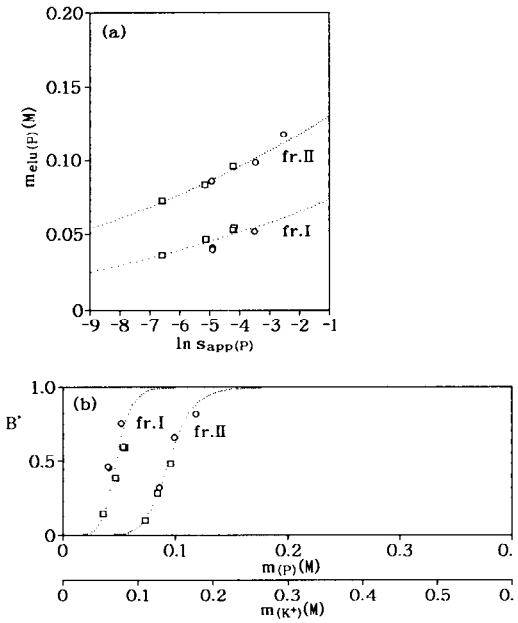

Fig. 6. Analysis of HPLC for IgG fractions I and II. Points in (a) and (b): experimental plots of (a) $m_{elu(P)}$ *versus* ln $s_{app(P)}$ and (b) B' *versus* $m_{(P)}$ or $m_{(K^+)}$ for two different $g'_{(P)}$ (ø = 1 cm) values: (○) 2.5 and (□) 0.45 mM/ml; the corresponding sample loads are 0.053–0.087 and 0.115–0.215 in units of absorbance (at 230 nm) × ml for any fraction. Other experimental conditions: $m_{in(P)}$ = 1 mM; flow-rate, 0.49–0.50 ml/min; P, 0.9–4.9 MPa; T, 20.0–25.0°C. Curves in (a) and (b): theoretical curves calculated by using (a) eqn. 6 and (b) eqn. 5; for details of the calculation method, see the legend for Fig. 4a–d.

the local molecular surface that effectively keeps in contact with the crystal surface of HA does not generally increase much with increase in molecular mass. Fig. 13 depicts the approximate molecular dimensions and shapes of both lysozyme and IgG; the arrangement of P sites on the **c** surface of HA is also shown on the same plane. It can be seen that the molecular shape of IgG is much more complicated than that of lysozyme, and that extreme ups and downs occur on the molecular surface of IgG; this would drastically reduce the x' value for IgG. In fact, it can be seen in Table I that the x' value, 11.0 (l.l. = 6.4; u.l. = 20.0), for "basic"IgG with large molecular dimensions does not increase much in comparison with the corresponding value, 5.7 (l.l. = 4.0; u.l. = 8.0), for lysozyme with small molecular dimensions. It is now useful to consider Fig. A6 in Appendix III in ref. 44 in which are presented photographs of space-filling models of poly-L-lysine and two sodium ions that are adsorbed on the **c** surface of HA. A visual image of the adsorption configuration of a protein molecule on the **c** surface of HA can be deduced from the photographs.

It can be seen in Table I that the x' value for "acidic" IgG, 18.0 (l.l. = 14.0; u.l. = 27.0) is larger than the corresponding value for "basic" IgG. This is compatible with the deduction (mentioned in the Introduction in PartIII[21]) that two C sites are present per unit cell on the **a** surface of HA whereas only a single P site is present per unit cell on the **c** surface.

It can also be seen in Table I that the x' values for ADP, ATP and adenosine

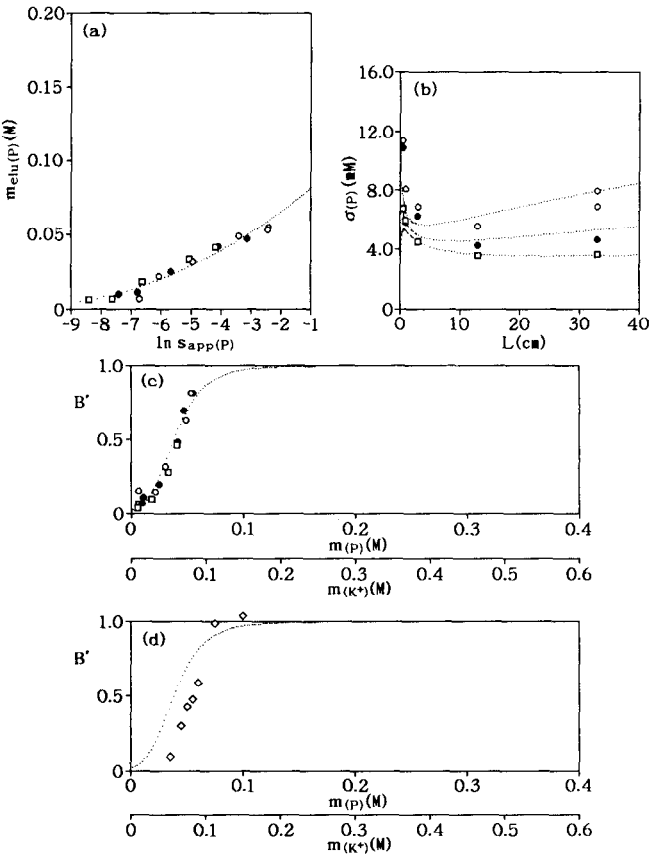

Fig. 7. Analysis of HPLC for BSA. Points in (a)–(c): experimental plots of (a) $m_{elu(P)}$ *versus* ln $s_{app(P)}$, (b) $\sigma_{(P)}$ *versus* L and (c) B' *versus* $m_{(P)}$ or $m_{(K^+)}$ for three different $g'_{(P)}$ (ø = 1 cm) values: (○) 2.5, (●) 1.25 and (□) 0.45 mM/ml; the corresponding sample loads are 120–480, 180–240 and 300–400 μg. Other experimental conditions: $m_{in(P)}$ = 1 mM; flow-rate, 0.46–0.51 ml/min; P, 0.3–5.3 MPa; T, 21.5–27.2°C. Curves in (a)–(c): theoretical curves calculated by using (a) eqn. 6, (b) eqn. 7 and (c) eqn. 5; for details of the calculation method, see the legend for Fig. 4a–d, where the parameters m, μ, etc., have been replaced with $m_{(p)}$, $m_{elu(P)}$, etc., by using eqns. 9–15, and not by using eqns. 9′–15′. Points in (d): experimental plots of B' *versus* $m_{(P)}$ or $m_{(K^+)}$, where B' values were estimated from isocratic chromatography carried out under the following experimental conditions: flow-rate, 0.49–0.50 ml/min; P, 1.6–3.9 MPa; T, 23.2–26.4°C. Curve in (d): theoretical curve identical with that shown in (c).

tetraphosphate are almost equal to one another, despite the expectation that x' should increase with increase in the number of phosphate groups that are involved in the polyphosphate chain (*cf.*, ref. 45). The constant x' value perhaps is associated with the degradation of the molecule occurring on the crystal surface of HA (*cf.*, refs. 1 and 45).

It is of interest that the standard deviation, $\sigma_{(P)}$, of the chromatographic peak for proteins in general decreases rapidly with increase in the total length, L, of the column, but that $\sigma_{(P)}$ increases slowly after the first rapid decrease (Figs. 4c, 5c and 7b). With ADP with a very small x' value (see Table I), however, the first rapid decrease in $\sigma_{(P)}$ does not occur (Fig. 9c). All these results have been obtained not only

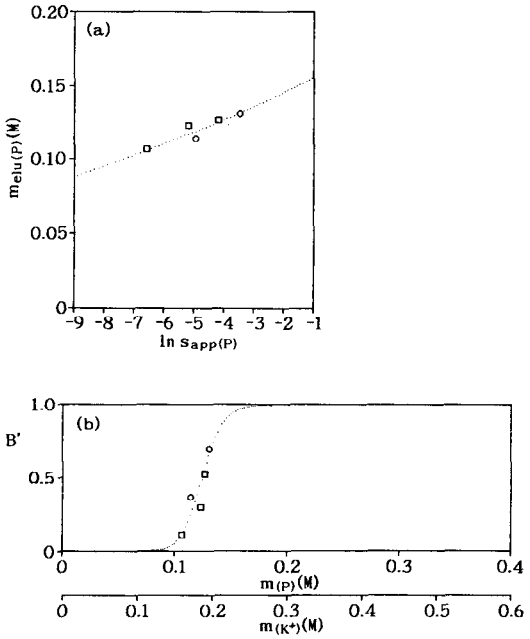

Fig. 8. Analysis of HPLC for IgG fraction III. Points in (a) and (b): experimental plots of (a) $m_{elu(P)}$ *versus* ln $s_{app(P)}$ and (b) B' *versus* $m_{(P)}$ or $m_{(K^+)}$ for two different $g'_{(P)}$ ($\varnothing = 1$ cm) values: (○) 2.5 and (□) 0.45 mM/ml; the corresponding sample loads are 0.047 and 0.062 in units of absorbance (at 230 nm) × ml. Other experimental conditions: $m_{in(P)}$ = 1 mM; flow-rate, 0.49–0.50 ml/min; P, 0.9–4.5 MPa; T, 21.6–24.5°C. Curves in (a) and (b): theoretical curves calculated by using (a) eqn. 6 and (b) eqn. 5; for details of the calculation method, see the legends for Fig. 4a–d and Fig. 7.

experimentally but also theoretically. Theoretically it can further be predicted that, with molecules with extremely large x' values, the first rapid decrease in $\sigma_{(P)}$ does not occur (*cf.*, Fig. 2 in ref. 46).

Finally, it appears that the experimental plots of B' *versus* $m_{(P)}$ or $m_{(K^+)}$ obtained on the basis of isocratic chromatography tend to deviate slightly from the corresponding plots obtained on the basis of gradient chromatography (*cf.*, Fig. 4d and e, Fig. 5d and e, Fig. 7c and d, and Fig. 9d and e, respectively). It can be assumed that this arises at least partially from the fact that the effective gradient participating in the competition mechanism in chromatography is not exactly linear even though a linear molarity gradient is applied. It is activity, and not molarity, that should be exactly linear with authentically linear gradient chromatography; on proposing the activity concept, account is taken of the interaction effect of competing ions occurring not only in the bulk solution but also on the crystal surface of HA (*cf.*, ref. 27).

Capacity factor, k', with the competition model

Provided that both the sample molecule and the competing ion are adsorbed weakly onto adsorbing sites while performing the competition, then the relationship $\varphi m \ll 1$ is fulfilled (*cf.*, explanation of φ in eqn. 5), and the approximate relationship

$$\varphi m + 1 \approx e^{\varphi m} \tag{16}$$

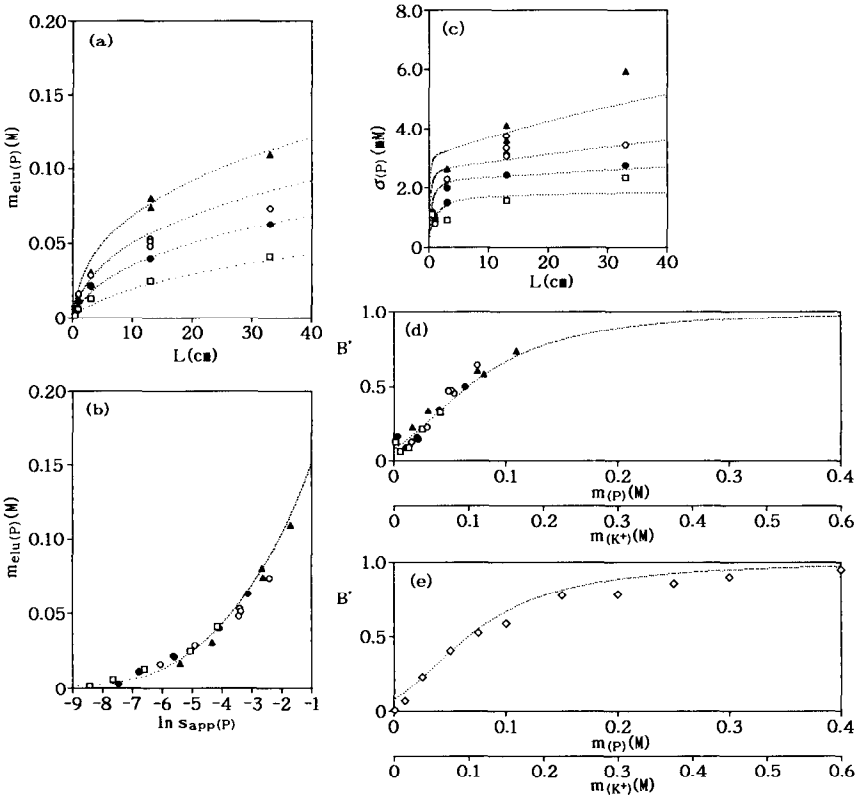

Fig. 9. Analysis of HPLC for ADP. Points in (a)–(d): experimental plots of (a) $m_{elu(P)}$ *versus* L, (b) $m_{elu(P)}$ *versus* ln $s_{app(P)}$, (c) $\sigma_{(P)}$ *versus* L and (d) B' *versus* $m_{(P)}$ or $m_{(K^+)}$ for four different $g'_{(P)}$ (ø = 1 cm) values: (▲) 5.0, (○) 2.5, (●) 1.25 and (□) 0.45 mM/ml; the corresponding sample loads are 0.9–4.0, ≲6, 1.7–10 and 5.5–15 μg. Other experimental conditions: $m_{in(P)}$ = 1 mM, flow-rate, 0.45–.051 ml/min; P, 0.3–5.2 MPa; T, 20.5–27.0°C. Curves in (a)–(d): theoretical curves calculated by using (a) eqn. 6, (b) eqn. 6, (c) eqn. 7 and (d) eqn. 5; for details of the calculation method, see the legends of Fig. 4a–d and Fig. 7. Points in (e): experimental plots of B' *versus* $m_{(P)}$ or $m_{(K^+)}$, where B' values were estimated from isocratic chromatography carried out under the following experimental conditions: flow-rate, 0.49–0.51 ml/min; P, 1.5–3.9 MPa; T, 25.0–29.5°C. Curve in (e): theoretical curve identical with that shown in (d).

holds. In this instance, eqn. 8 can be rewritten as

$$\ln k'(m) \approx -x'\varphi m + \ln q \tag{17}$$

indicating that ln $k'(m)$ decreases linearly with increase in m.

In contrast, provided that both the sample molecule and the competing ion are

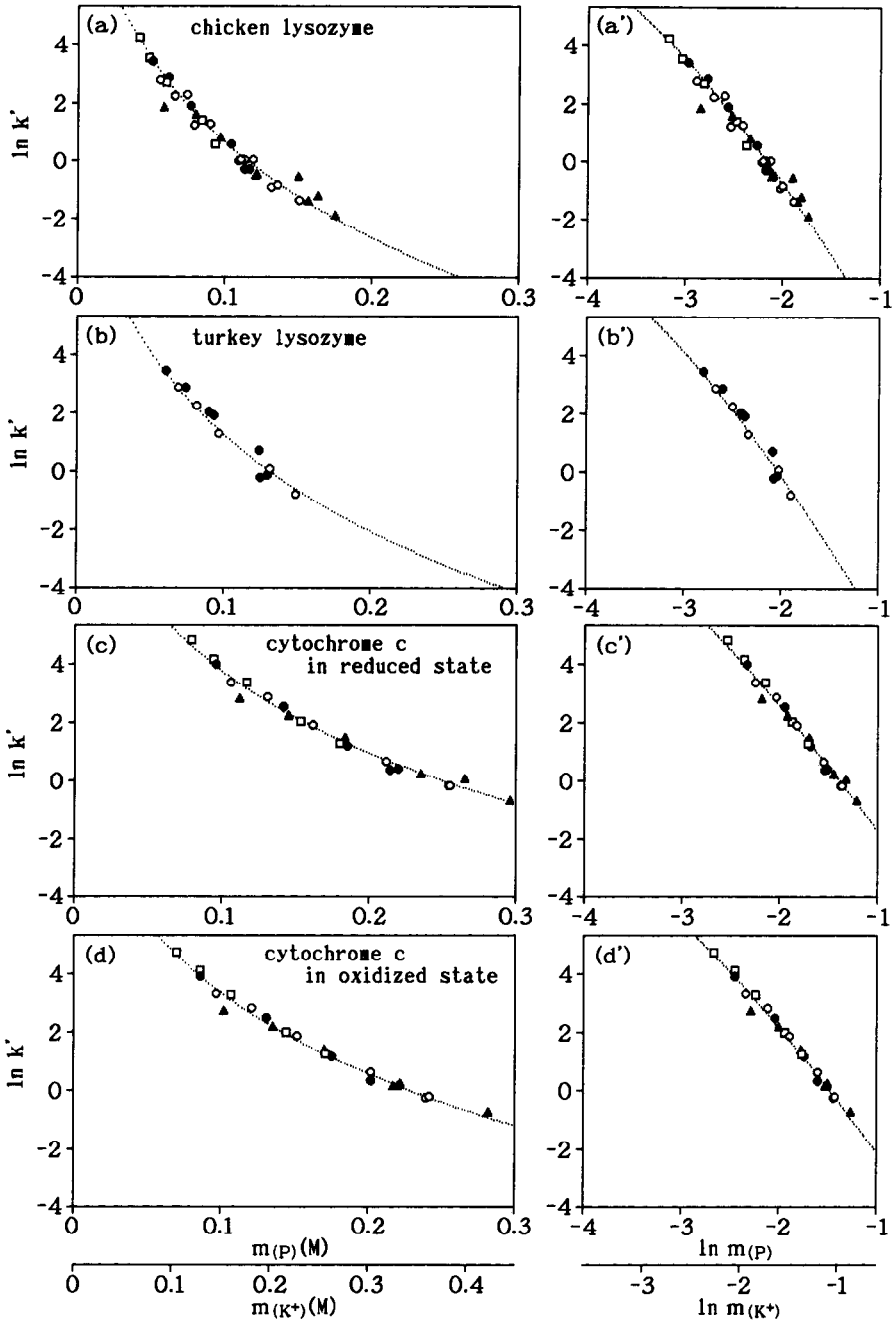

Fig. 10.

(Continued on p. 114)

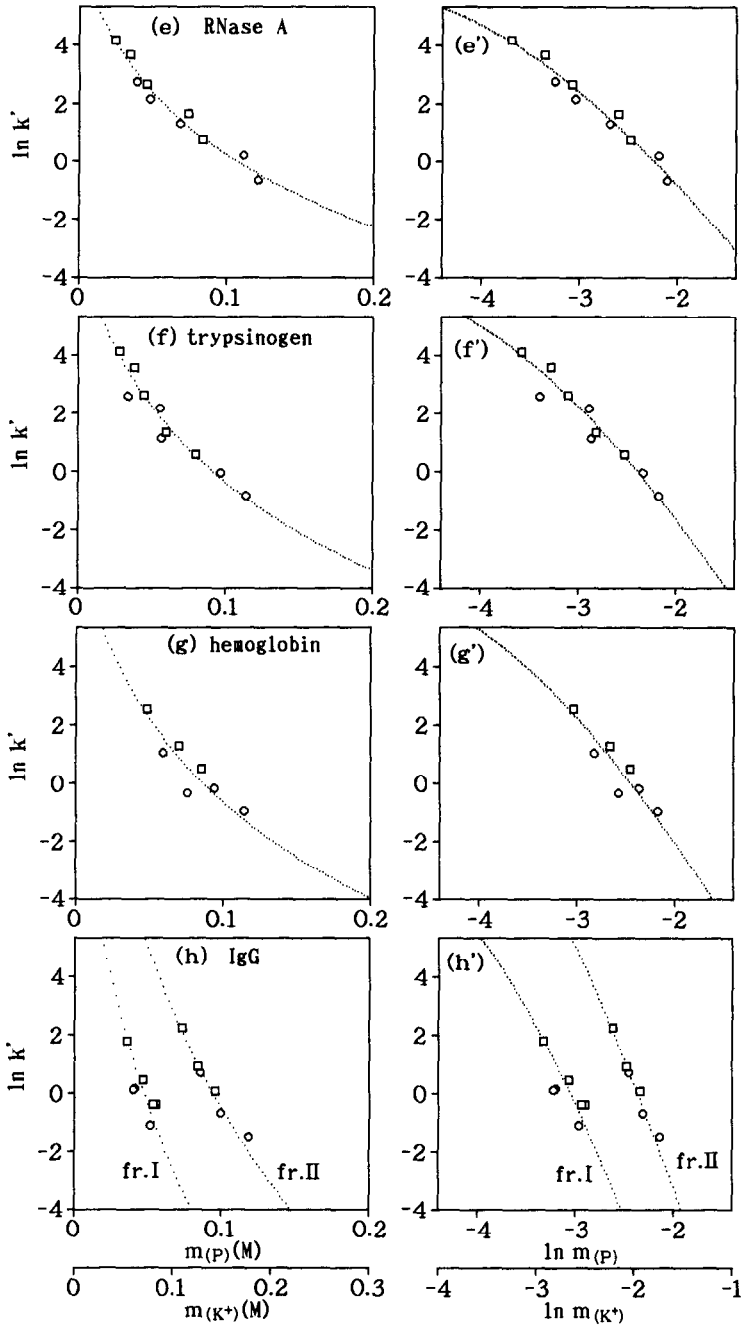
(e) RNase A
(e')
(f) trypsinogen
(f')
(g) hemoglobin
(g')
(h) IgG
(h')
ln k'
fr.I
fr.II
m(P)(M)
m(K+)(M)
ln m(P)
ln m(K+)

Fig. 10.

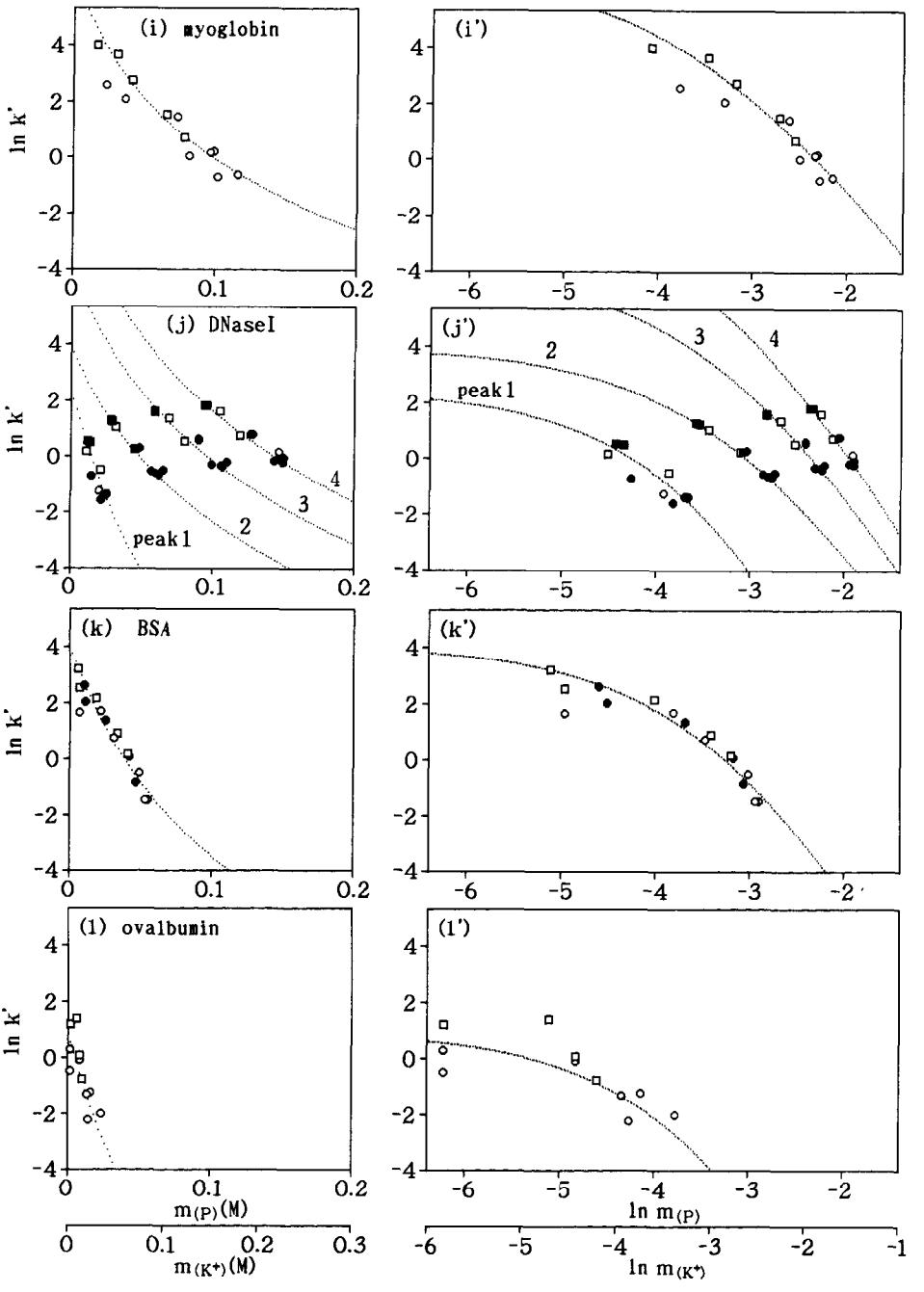

Fig. 10.

(Continued on p. 116)

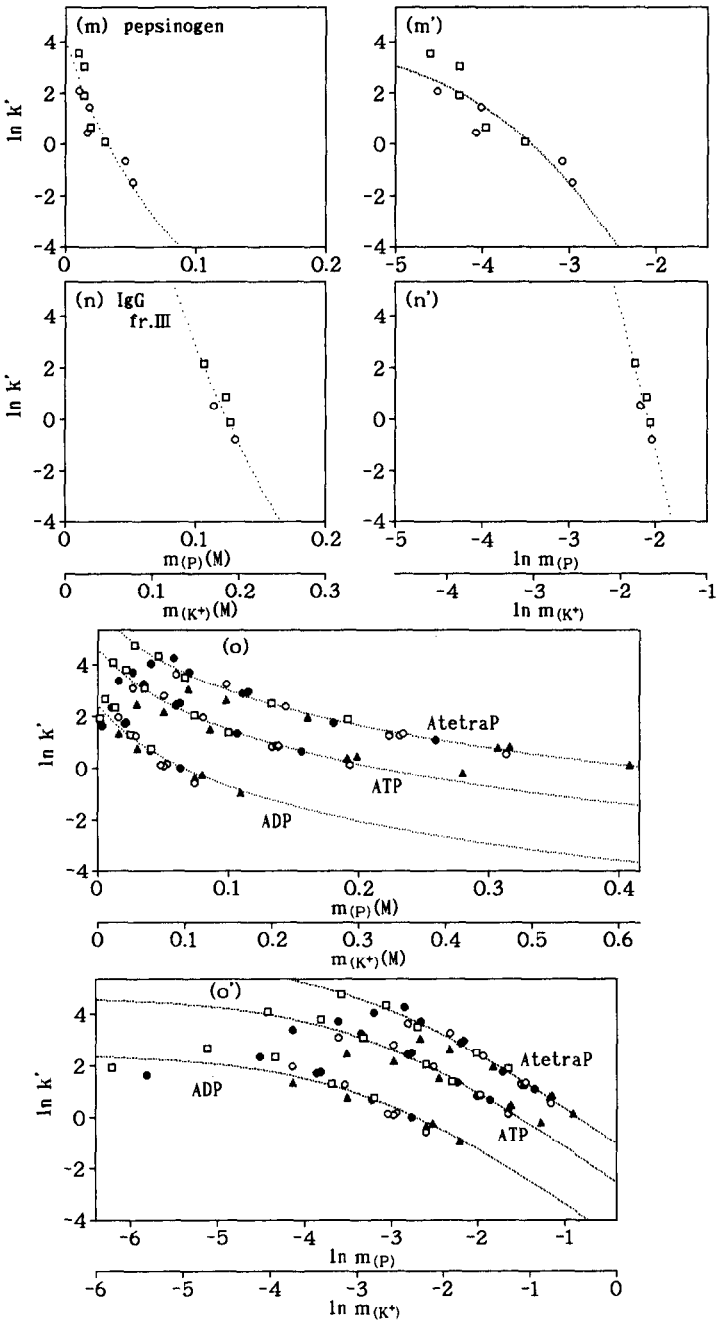

Fig. 10. Points: experimental plots of ln k' *versus* $m_{(P)}$ or $m_{(K^+)}$ (a–o) and ln k' *versus* ln $m_{(P)}$ or ln $m_{(K^+)}$ (a'–o'). All the experiments were carried out between 20.0 and 29.7°C, and the symbols ▲, ○, ●, □ and ■ correspond to the experiments performed by using $g'_{(P)}$ (ø = 1 cm) values of 5.0, 2.5, 1.25, 0.45 and 0.15 mM/ml, respectively. Curves: theoretical curves calculated by using eqn. 8.

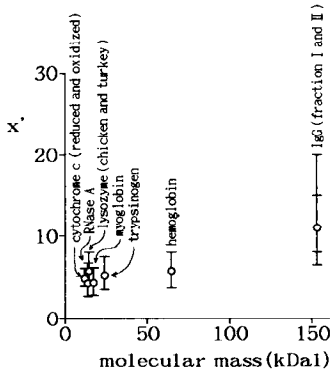

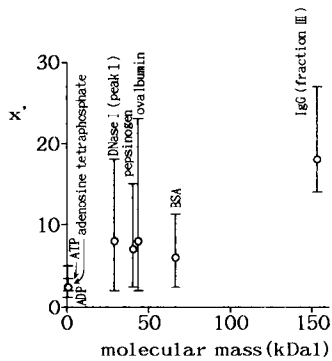

Fig. 11. Plots of x' *versus* molecular mass for "basic" proteins shown in Table I. kDal = kilodalton.

Fig. 12. As Fig. 11 for "acidic" substances shown in Table I.

adsorbed strongly onto adsorbing sites, then the relationship $\varphi m \gg 1$ is fulfilled (*cf.*, explanation of φ in eqn. 5), and the approximate relationship

$$\varphi m + 1 \approx \varphi m \tag{18}$$

holds. In this instance, eqn. 8 can be rewritten as

$$\begin{aligned} \ln k'(m) &\approx -x' \ln m + \ln q - x' \ln \varphi \\ &= -x' \ln m + \ln \kappa \end{aligned} \tag{19}$$

(*cf.*, eqn. A2 in Appendix I), indicating that $\ln k'(m)$ decreases linearly with increase in $\ln m$.

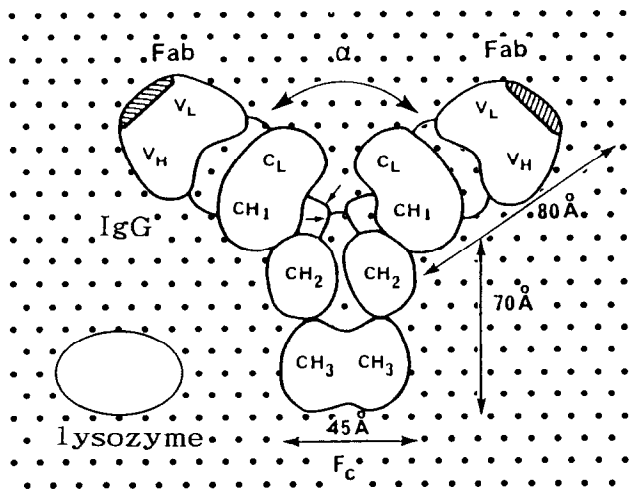

Fig. 13. Approximate molecular dimensions and shapes of lysozyme and IgG, and the arrangement of P sites on the c surface of HA; for the arrangement of P sites, see Part III[21]. (Reproduced with modifications from refs. 35 and 43.)

It can be seen in Fig. 10 that the arrangement of the experimental points on the $\{m_{(P)}$ [or $m_{(K^+)}$], ln $k'\}$ and the $\{\ln m_{(P)}$ [or ln $m_{(K^+)}$], ln $k'\}$ plane, in general, deviates slightly from linearity, being concave and convex, respectively. This indicates that the adsorption of competing ions (and also that of sample molecules) onto crystal sites of HA is not extremely weak or extremely strong; it is eqn. 8, rather than eqn. 17 or 19, that coincides best with the experiment.

It should be recalled that the best theoretical curve on the [ln $s_{app(P)}$, $m_{elu(P)}$] plane was used as calibration graph for the determination of the arrangement of the experimental points on the $\{m_{(P)}$ [or $m_{(K^+)}$], $B'\}$ plane (last sub-section of Experimental and Results). This means that the arrangement of the experimental points on both $\{m_{(P)}$ [or $m_{(K^+)}$], ln $k'\}$ and $\{\ln m_{(P)}$ [or ln $m_{(K^+)}$], ln $k'\}$ planes depends on the theoretical calibration graph that has been chosen on the [ln $s_{app(P)}$, $m_{elu(P)}$] plane. It has been confirmed, however, that the dependence occurs only very slightly, and that the arrangement of the experimental points on the $\{m_{(P)}$ [or $m_{(K^+)}$], $B'\}$, $\{m_{(P)}$ [or $m_{(K^+)}$], ln $k'\}$ or $\{\ln m_{(P)}$ [or ln $m_{(K^+)}$], ln $k'\}$ plane is almost constant, unless the theoretical calibration graph on the [ln $s_{app(P)}$, $m_{elu(P)}$] plane deviates substantially from the experimental plot.

APPENDIX I

Evaluation of the lower and upper limit, $x'_{l.l.}$ and $x'_{u.l.}$, of the parameter x' (cf., Table I)

The theoretical curve (eqn. 6) mapped on the (ln s, μ) or the [ln $s_{app(P)}$, $m_{elu(P)}$] plane has the following properties when ln s or ln $s_{app(P)}$ varies within the range that is usually applied:

(a) Except when $x' = \infty$ [*cf.*, (c)], the curve is slightly concave with positive tangential slopes.

(b) The curve performs a parallel transition towards the left when the parameter q or $q_{app(P)}$ increases.

(c) The mean tangential slope, $\bar{G}$, of the curve decreases when the parameter x' increases. When x' approaches infinity, $\bar{G}$ tends to zero, and the curve reduces to a straight line that is parallel to the ln s or the ln $s_{app(P)}$ axis.

(d) $\bar{G}$ also decreases when the parameter φ increases. When φ approaches infinity, $\bar{G}$ tends to a finite limiting value, $\overline{G^0}_{x'}$, which depends upon x' [*cf.*, (g)].

(e) It is possible to keep $\bar{G}$ constant either by increasing φ and decreasing x' at the same time, or by decreasing φ and increasing x' at the same time [*cf.*, (c) and (d)]. If q or $q_{app(P)}$ is increased appropriately while performing the former operation, or if q or $q_{app(P)}$ is decreased appropriately while performing the latter operation, then the position of the curve can be kept constant [*cf.*, (b)].

(f) When φ increases and x' decreases under the condition of a constant $\bar{G}$ [*cf.*, (e)], then the curvature of the curve increases. Especially if φ approaches infinity and x' tends to a finite value, x'_0, while holding the relationship of $q^{1/x'} = O(\varphi)$, then both the curvature (*i.e.*, the shape) and the position of the curve are stabilized. This can be understood from the fact that, at this limit, eqn. 6 converges to

$$\mu(s) = [(x'_0 + 1)\,\kappa s + {m_{in}}^{x'_0+1}]^{1/(x'_0+1)} \tag{A1}$$

in which

$$\kappa = q\varphi^{-x'_0} \tag{A2}$$

represents a constant with a finite value.

(g) $\overline{G^0}_{x'}$ [*cf.*, (d)] increases when x' decreases. (The increase in $\overline{G^0}_{x'}$ occurs mainly due to the increase in tangential slopes of the right-hand part of the curve.)

The lower and the upper limit of the possible x' values (written as $x'_{l.l.}$ and $x'_{u.l.}$, respectively) can be estimated on the basis of the experimental plot of $m_{elu(P)}$ *versus* ln $s_{app(P)}$. Thus, both $x'_{l.l.}$ and $x'_{u.l.}$ are involved in the combinations of (x', φ) that equalize the theoretical $\bar{G}$ with the experimental $\bar{G}$ while adjusting $q_{app(P)}$ or ln $q_{app(P)}$ in order for the theoretical curve to be superimposed on the experimental plot at least partially [*cf.*,(e)]. $x'_{l.l.}$ and $x'_{u.l.}$ are represented by the maximum and the minimum x' that give the theoretical curve a curvature stronger and weaker than that for the experimental plot, respectively [*cf.*, (f)].

It often happens, however, that, when $x' < x'_{u.l.}$, the curvature of the theoretical curve increases only slightly with both the decrease in x' and the increase in φ. Further, the shape and the position of the curve are both stabilized rapidly when φ approaches infinity and x' tends to $x'_0 + 0$ while holding the relationship of $q^{1/x'} = O(\varphi)$ [*cf.*, (f)]. In this instance, the curvature of the theoretical curve obtained when $x' = x'_{u.l.}$ is almost equal to that obtained when $x' = x'_0$, and it can be considered that $x'_0 = x'_{l.l.}$. [If x' decreases from $x'_{l.l.}$, then $\overline{G^0}_{x'}$ increases, *i.e.*, $\overline{G^0}_{x'}$ deviates from the experimental $\bar{G}$; *cf.*, (g).]

The points in Fig. 14 are experimental plots of $m_{elu(P)}$ *versus* ln $s_{app(P)}$ for chicken lysozyme (reproduced from Fig. 4b). Curves 1–4 are theoretical, calculated by using eqn. 6 or A1 where it has been assumed that [x', φ, ln $q_{app(P)}$] = (14.0, 4.0 M^{-1}, 7.1); (8.0, 10.0 M^{-1}, 7.9); (5.7, 25.0 M^{-1}, 9.5); and (4.0, ∞ M^{-1}, ∞), with ln $\kappa_{app(P)} \equiv$ ln κ + ln $q_{app(P)}$ − ln q (= ln κ + ln 0.970; see eqn. 15′) = −7.0, respectively (for κ, see eqn. A2). On the basis of the assumptions, both the mean tangential slopes $\bar{G}$ (or $\overline{G^0}_{x'}$) and the positions of the theoretical curves 1–4 are almost equal to those for the experimental plot. Further, if $x' \leqslant 5.7$, the curvature of the theoretical curve is similar to that for the experimental plot (curves 3 and 4). If $x' = 14$, however, the curvature of the theoretical curve is evidently less strong than that for the experimental plot (curve 1), from which it

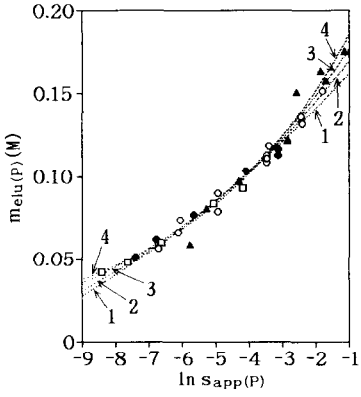

Fig. 14. Points: experimental plots of $m_{elu(P)}$ *versus* ln $s_{app(P)}$ for chicken lysozyme, reproduced from Fig. 4b. Curves 1–4: theoretical curves calculated by using eqn. 6 or A1 where it was assumed that [x', φ, ln $q_{app(P)}$] = (14.0, 4.0 M^{-1}, 7.1); (8.0, 10.0 M^{-1}, 7.9); (5.7, 25.0 M^{-1}, 9.5); and (4.0, ∞ M^{-1}, ∞), respectively, with ln $\kappa_{app(P)}$ = −7.0. For details, see text.

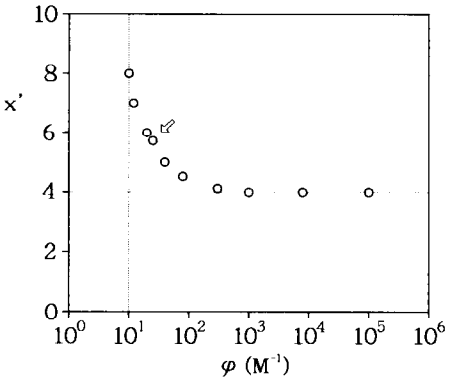

Fig. 15. Plots of x' *versus* φ for chicken lysozyme, where both x' and φ values were obtained from the optimum combinations of x', φ and ln $q_{app(P)}$. The vertical and horizontal dotted lines represent the lower limit value of φ and the x'_0 value, respectively. The point indicated by the arrow corresponds to the value of φ, 25 M^{-1}.

can be calculated that $x'_{u.l.} \approx 8.0$ (curve 2). $x'_{l.l.}$ can be represented by x'_0, and it can be estimated that $x'_{l.l.} = 4.0$ (curve 4).

The points in Fig. 15 are plots of x' *versus* φ for chicken lysozyme; both x' and φ values have been taken from the best combinations of x', φ and ln $q_{app(P)}$, three of which correspond to curves 2–4 in Fig. 14. In Fig. 15, the vertical and horizontal dotted lines represent the lower limit value of φ and the x'_0 value, respectively; the point indicated by the arrow corresponds to the value of φ, 25 M^{-1}. It can be seen in Fig. 15 that the x' value corresponding to $\varphi = 25$ M^{-1} represents a reasonable mean x' value.

For substances other than chicken lysozyme, plots similar to that shown in Fig. 15 can also be obtained. In some instances, however, it can clearly be shown that $x'_{l.l.} > x'_0$. A value of φ of 25 M^{-1} generates reasonable mean x' values for all substances.

APPENDIX II

Fractions I, II and III of IgG

Fig. 16 illustrates a double gradient chromatogram of IgG. This was obtained by previously applying a KCl gradient after an isocratic elution with 10 mM KP; 10 mM

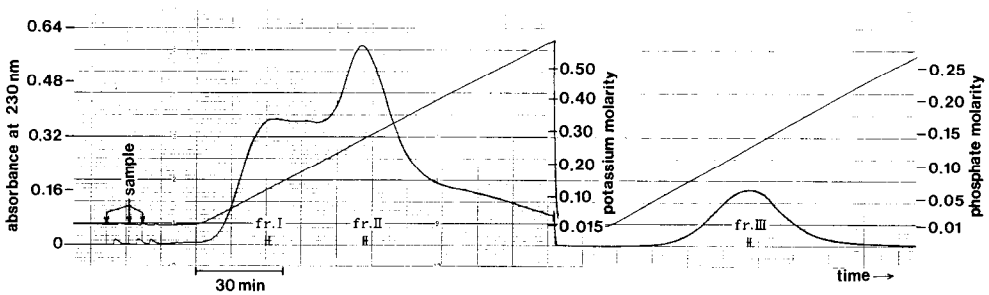

Fig. 16. Double gradient chromatogram for IgG (27 mg) as obtained on the KB column packed with HA type S_1; column 5 cm × 2 cm I.D. Experimental conditions: $m_{in(P)} = 10$ mM for both KCl and KP gradients; $g'_{(KCl)}$ (ø = 1 cm) = 3.75 mM/ml; $g'_{(P;KP)}$ (ø = 1 cm) = 2.5 mM/ml; flow-rate, 5.04 ml/min; P, 3.2–3.5 MPa; T, 24.0°C; recovery = 118%; 10 mM KP is always present in the KCl gradient.

KP was present while the KCl gradient continued (left-hand side of Fig. 16). The carrier solvent was again replaced with pure 10 m*M* KP, and the KP gradient was finally applied (right-hand side of Fig. 16). It can be seen that IgG is eluted partially in the first KCl gradient and partially in the second KP gradient. It can be considered (see Introduction) that IgG components that are eluted in the first and the second gradients behave as "basic" and "acidic" molecules, respectively, on the HA column. Therefore, of fractions I, II and III (see Fig. 16) that are used for the experiment (see Table I), both fractons I and II are assemblies of "basic" molecules; fraction III is an assembly of "acidic" molecules.

APPENDIX III

Relationship with the isoelectric point

In the Introduction, the correlation between the isoelectric point (p*I*) and the μ [or $m_{elu(P)}$] value for 26 proteins is argued (see Fig. 2). The same argument will be made in Part III[21] for the proteins listed in Table I (see Fig. 7 in ref. 21).

Eqn. 5 shows that the molarity, $\dot{m}$, of competing ions at which $B' = 1/2$ is given by

$$\dot{m} = (q^{1/x'} - 1)/\varphi \tag{A3}$$

and, in general, it is more reasonable to consider the correlation between p*I* and $\dot{m}$ [or $\dot{m}_{(P)}$] than the correlation between p*I* and μ [or $m_{elu(P)}$] [for $\dot{m}_{(P)}$, see below].

The points in Fig. 17 are plots of $\dot{m}_{(P)}$ *versus* $m_{elu(P)}$ for the substances listed in

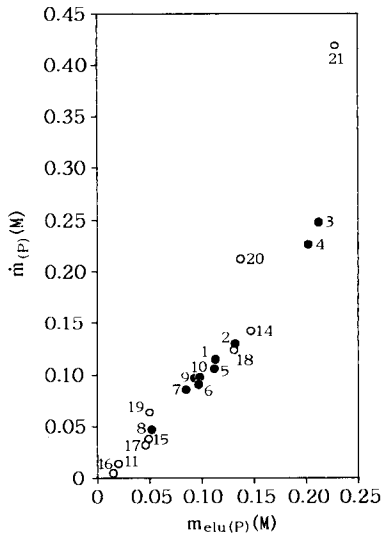

Fig. 17. Plots of $\dot{m}_{(P)}$ *versus* $m_{elu(P)}$ for the substances listed in Table I, where $m_{elu(P)}$ represents the elution molarity obtained when L = 13 cm and $g'_{(P)}$ ($\varnothing$ = 1 cm) = 2.5 m*M*/ml. The numbers against the experimental points are the numbers of the substances given in the first column in Table I; ○ and ● correspond to "acidic" and "basic" molecules, respectively.

Table I, where $\dot{m}_{(P)}$ is related to $\dot{m}$ by the relationships $\dot{m} = \dot{m}_{(P)}$ and $\dot{m} = 1.5\dot{m}_{(P)}$ for "acidic" and "basic" molecules respectively (*cf.*, eqns. 9 and 9'); $m_{elu(P)}$ here represents othe elution molarity obtained when $L = 13$ cm and $g'_{(P)}(\text{ø} = 1\text{ cm}) = 2.5\ \text{m}M/\text{ml}$, *i.e.*, when $s_{app(P)} = 32.5\ \text{m}M/\text{cm}^2$. It can be seen in Fig. 17 that $\dot{m}_{(P)}$ is highly correlated with $m_{elu(P)}$ with respect to proteins. The correlation between p*I* and $\dot{m}$ [or $\dot{m}_{(P)}$] with proteins can therefore be replaced by the correlation between p*I* and μ [or $m_{elu(P)}$] for practical purposes.

REFERENCES

1 T. Kawasaki, *J. Chromatogr.*, submitted for publication.
2 A. Tiselius, S. Hjertén and Ö. Levin, *Arch. Biochem. Biophys.*, 65 (1956) 132.
3 G. Bernardi, *Methods Enzymol.*, 21 (1971) 95.
4 G. Bernardi, *Methods Enzymol.*, 22 (1971) 325.
5 G. Bernardi, *Methods Enzymol.*, 27 (1973) 471.
6 B. Moss and E. N. Rosenblum, *J. Biol. Chem.*, 247 (1972) 5194.
7 H. G. Martinson, *Biochemistry*, 12 (1973) 139.
8 H. G. Martinson and E. B. Wagenaar, *Biochemistry*, 13 (1974) 1641.
9 M. Spencer, *J. Chromatogr.*, 166 (1978) 423.
10 M. Spencer, *J. Chromatogr.*, 166 (1978) 435.
11 M. J. Gorbunoff, *Anal. Biochem.*, 136 (1984) 425.
12 M. J. Gorbunoff, *Anal. Biochem.*, 136 (1984) 433.
13 M. J. Gorbunoff and S. N. Timasheff, *Anal. Biochem.*, 136 (1984) 440.
14 T. Kawasaki, S. Takahashi and K. Ikeda, *Eur. J. Biochem.*, 152 (1985) 361.
15 T. Kawasaki, K. Ikeda, S. Takahashi and Y. Kuboki, *Eur. J. Biochem.*, 155 (1986) 249.
16 T. Kawasaki, W. Kobayashi, K. Ikeda, S. Takahashi and H. Monma, *Eur. J. Biochem.*, 157 (1986) 291.
17 T. Kawasaki, M. Niikura, S. Takahashi and W. Kobayashi, *Biochem. Int.*, 13 (1986) 969.
18 T. Kadoya, T. Isobe, M. Ebihara, T. Ogawa, M. Sumita, H. Kuwahara, A. Kobayashi, T. Ishikawa and T. Okuyama, *J. Liq. Chromatogr.*, 9 (1986) 3543.
19 Y. Kato, K. Nakamura and T. Hashimoto, *J. Chromatogr.*, 398 (1987) 340.
20 T. Kawasaki and W. Kobayashi, *Biochem. Int.*, 14 (1987) 55.
21 T. Kawasaki, M. Niikura and Y. Kobayashi, *J. Chromatogr.*, 515 (1990) 125.
22 T. Kawasaki, M. Niikura, S. Takahashi and W. Kobayashi, *Biochem. Int.*, 15 (1987) 1137.
23 T. Sato, T. Okuyama, T. Ogawa and M. Ebihara, *Bunseki Kagaku*, 38 (1989) 34.
24 R. Kasai, H. Yamaguchi and O. Tanaka, *J. Chromatogr.*, 407 (1987) 205.
25 T. Kawasaki, *Sep. Sci. Technol.*, 23 (1988) 601.
26 T. Kawasaki, *Sep. Sci. Technol.*, 23 (1988) 617.
27 T. Kawasaki, *Sep. Sci. Technol.*, 23 (1988) 1105.
28 G. Bernardi, M. G. Giro and C. Gaillard, *Biochim. Biophys. Acta*, 278 (1972) 409.
29 T. Isobe and T. Okuyama, *Kagaku*, Suppl., 102 (1984) 141.
30 T. Kawasaki, *Sep. Sci. Technol.*, 22 (1987) 121.
31 T. Kawasaki, *Sep. Sci. Technol.*, 23 (1988) 451.
32 T. Kawasaki, *Sep. Sci. Technol.*, 23 (1988) 2365.
33 T. Kawasaki, *Sep. Sci. Technol.*, 24 (1989) 1109.
34 T. Kawasaki and M. Niikura, *Sep. Sci. Technol.*, 25 (1990) in press.
35 T. Kawasaki, *J. Chromatogr.*, 93 (1974) 313.
36 T. Kawasaki, *Sep. Sci. Technol.*, 16 (1981) 439.
37 T. Kawasaki and S. Takahashi, *Sep. Sci. Technol.*, 23 (1988) 193.
38 T. Kawasaki, *Sep. Sci. Technol.*, 17 (1982) 407.
39 J. C. Giddings, *Dynamics of Chromatography: Part I, Principles and Theory*, Marcel Dekker, New York, 1965, p. 13.
40 T. Kawasaki, *Biopolymers*, 9 (1970) 277.
41 T. Kawasaki, *J. Chromatogr.*, 93 (1974) 337.

42 T. Kawasaki and G. Bernardi, *Biopolymers*, 9 (1970) 257.
43 R. E. Cathou, in G. W. Litman and R. A. Good (Editors), *Immunoglobulins*, Plenum Press, New York and London, 1978, p. 37.
44 T. Kawasaki, *J. Chromatogr.*, 157 (1978) 7.
45 T. Kawasaki, *J. Chromatogr.*, 151 (1978) 95.
46 T. Kawasaki, *Sep. Sci. Technol.*, 16 (1981) 439.